MODAL CHARACTERIZATION OF THE ASCIE SEGMENTED OPTICS TEST BED: NEW ALGORITHMS AND EXPERIMENTAL RESULTS

Alain CARRIER, Jean-Noel AUBRUN
Lockheed Palo-Alto Research Laboratory, 1801 Page Mill Road,
Building 250, Organization 92-30, Palo-Alto, California, 94304-1211
Tel: (415) 354-5987 FAX (415) 354-5638

February 21, 1992

Abstract

New frequency response measurement procedures, on-line modal tuning techniques, and off-line modal identification algorithms are developed and applied to the modal identification of the Advanced Structures/Controls Integrated Experiment (ASCIE), a generic segmented optics telescope test-bed representative of future complex space structures.

The frequency response measurement procedure uses all the actuators simultaneously to excite the structure and all the sensors to measure the structural response so that all the transfer functions are measured simultaneously. Structural responses to sinusoidal excitations are measured and analyzed to calculate spectral responses. The spectral responses in turn are analyzed as the spectral data become available and, which is new, the results are used to maintain high quality measurements. Data acquisition, processing, and checking procedures are fully automated.

As the acquisition of the frequency response progresses, an on-line algorithm keeps track of the actuator force distribution that maximizes the structural response to automatically tune to a structural mode when approaching a resonant frequency. This tuning is insensitive to delays, ill-conditioning, and nonproportional damping. Experimental results show that it is useful for modal surveys even in high modal density regions.

For thorough modeling, a constructive procedure is proposed to identify the dynamics of a complex system from its frequency response with the minimization of a least-squares cost function as a desirable objective. This procedure relies on off-line modal separation algorithms to extract modal information and on least-squares parameter subset optimization to combine the modal results and globally fit the modal parameters to the measured data. The modal separation algorithms resolved modal density of 5 modes/Hz in the ASCIE experiment. They promise to be useful in many challenging applications.

Keywords: *modal characterization, system identification, flexible structures, segmented optics*

0 BACKGROUND

Active control for large flexible structures has been the object of 15 years of research, yet because of the lack of experimental demonstrations traceable to actual developments, it has not been im-

plemented in a single space mission. Much work has been done on not so large and not so complex flexible structures. As a result, numerically tractable and numerically robust procedures and algorithms for modeling and high performance control of truly large and complex systems are lacking. Precision segmented reflectors are major examples of systems where the size and the complexity issues arise. The Keck Ten Meter Telescope, soon to be operational on Mount Mauna Kea in Hawaii, is one of them. The Keck primary mirror is composed of 36 hexagonal segments. The control system uses 108 actuators and 162 sensors to maintain the segments optically aligned. The Keck structure has 150 modes below 50 Hz with a modal density as high as 25 modes/Hz. Regrettably, the Keck telescope will not benefit from structural control technology.

To address the challenges specific to the active control of precision segmented optics, and to the active control of complex flexible structures in general, the Lockheed Palo-Alto Research Laboratory designed and built the Advanced Structures/Controls Integrated Experiment (ASCIE). The ASCIE test-bed emulates a telescope with a segmented mirror. Its seven-hexagonal-segment primary mirror is mounted on a lightweight flexible truss structure. The six peripheral segments are actively controlled by 18 electromagnetic precision actuators. 24 position sensors measure the relative displacements between the segments. The ASCIE segmented optics and support structure have 50 modes below 50 Hz. The ASCIE control hardware [1] which has been designed to meet the strict requirements for precision control of segmented optics has demonstrated segment alignment performance down to 60 nanometers rms. Using a non validated Finite Element Model and worst case control design techniques, a factor of 3 to 5 improvement in segment alignment bandwidth was achieved over classical control techniques, and vibration attenuation in 25 out of 28 controlled modes was experimentally demonstrated.

The objective of the present work is to develop a dynamic model of ASCIE from experimental input output data. The objective is twofold. One objective is to test how accurately the dynamic behavior of complex systems like ASCIE can be predicted by Finite Element Analysis (one to one comparison between the Finite Element and the identified models requires careful system identification to extract all the natural modes of the system including those with relatively low response). The other is to develop a control design model. This model will be used to test how much improvement in segment alignment bandwidth and structural vibration suppression is achievable using an identified versus an FEM model. This paper reports on our work in modeling ASCIE.

1 INTRODUCTION

In this paper, a new modal characterization technique is developed. It identifies structural modes by applying the principles of gain (singular value) analysis during both the on-line data acquisition, and the off-line parametric identification processes.

The new characterization technique is applied to identify the dynamic model of the ASCIE segmented optics test bed. It coped successfully with the enormous task of estimating more than 2000 modal parameters. 50 modes were identified. The modes come primarily in two dense clusters: one cluster in a 5 Hz frequency band contains 18 modes; the other in an 8 Hz frequency band contains 12 modes. The ASCIE high modal density structure is representative of complex space structures.

For large flexible structures, present characterization techniques do not provide a reliable strategy to collect response data that have information about all of the dynamics of the test article, and

they become numerically untractable when it comes to extracting the dynamic information from the test data, particularly when the data is rich in modal information in some frequency bands [2].

To properly excite all of the dynamics of a large structure, wide-band random excitations, or impulse excitations requires levels of energy that would alter the integrity of the structure. Therefore, unless new excitations strategies are found, the Total Least Square [3] and the Eigenvalue Realization Algorithm [4] which are, at present, two popular identification techniques based on these types of test signals, as well as many other techniques, will only find limited engineering applications.

With system size blowing out the work space and the processing time requirements, and high modal density introducing numerical ill-conditioning, extracting the dynamic information from the test data for large structures is a computationally challenging task. The size, a function of the number of inputs, number of outputs, and number of modes, is a critical factor as the amount of data to be processed can exceed the work space of most current computers. On actual hardware, identification techniques have so far only been demonstrated on relatively small size systems [5], [6]. At present, no technique has addressed the computational complexity associated with high modal density structures.

When they do not require prohibitive testing time, classical sinusoidal or multitone excitations can be used to systematically excite all of the dynamics of a test article [7], [8], [9]. For these test signals, the characterization task is one of fitting a linear time invariant model to a measured non parametric complex admittance matrix. This is known to be a difficult task, and even the most recent single-input single-output, or single-input multiple-output fitting techniques exhibit serious numerical problems for relatively simple systems [10]. For high modal density structures, these techniques would be inappropriate because they would fail to differentiate natural vibration modes. The problem of modeling dynamic systems from their measured frequency responses has motivated some new efforts in rational interpolation theory [11], [12], [13], but whether these efforts effectively address the practical issues has still to be demonstrated.

Our work was to explore new excitation techniques for data acquisition using sinusoidal test signals, and new algorithms for extracting modal information from the non-parametric frequency response test data.

The data acquisition process we tested is classical, but the way we implemented it is not. Steady state responses to sinusoidal excitations were analyzed to determine the system admittance matrix at a given frequency, and frequency sweep was used to determine the full non parametric frequency dependent system admittance matrix. System non-linearities were handled via harmonic analysis. But, with what is new at each frequency, a system inversion was approximately realized to achieve good signal to noise ratio. In addition, the principal system admittance gains and associated input and output patterns were determined. This approach yields some important and inherently multivariable properties of the system being tested: namely, the modal frequencies, the modal dampings, what is new, and the mode shapes because, at a resonant frequency, the maximum system admittance gain is obtained when the actuator inputs are combined so as to excite a pure mode. Dwells in both spatial and frequency domains are performed which is critical to the modal identification of complex symmetric lightly damped structures, since for such structures tuning to the resonant frequency alone fails to isolate closely spaced modes.

When the acquisition process was completed, a parametric modal model was fitted to the full non parametric measured system admittance matrix, and new algorithms based on low rank matrix

approximation, or on convex and quadratic optimization techniques were used to carry one step further the identification of the modal parameters started during the data acquisition process. The algorithms are used repeatedly. Each time they are called, they extract one or several dominant natural modes from the non parametric response over a prespecified frequency range. To identify a mode, they use the modal information contained in the maximum system admittance gain and its associated input and output patterns, and the consistency of this modal information over any specified frequency range to give accurate modal parameters free to the extent possible from the contributions of the nearby modes.

The paper is organized as follows. Section 2 describes the ASCIE high modal density flexible structure that was used to demonstrate the new modeling techniques. In section 3, we discuss some of the issues involved in gathering a good set of input-output data for modeling complex flexible structures. In section 4, measured frequency response data are used to explore some of the difficulties associated with the modal characterization of the ASCIE segmented optics test-bed, and to define a sensible optimization criterion for parametric identification. In section 5, we discuss the choice of a model for flexible structures and modal testing under various assumptions. Section 6 addresses our work in data acquisition and on-line modal testing, and its application to the ASCIE experiment. Section 7 addresses our work in off-line modal analysis, in model refinement via parameter optimization, and its application to the modal identification of ASCIE.

2 ASCIE TEST-BED

The ASCIE emulates an f/1.25 Cassegrain telescope.* Its seven-hexagonal-segment primary mirror is mounted on a lightweight flexible truss structure. The six peripheral segments are actively controlled in three degrees of freedom by 18 linear electromagnetic precision actuators. 24 Kaman position sensors (4 per actively controlled segment) are used to measure the relative displacements between the segments and generate commands for the actuators to keep the segments optically aligned, the central segment acting as a reference.

Non Colocated sensing: The edge inductance sensors measure the relative positions of the primary mirror segments. The central segment, instead of the support structure which lacks dimensional stability, is used as a reference. The edge sensors have a 60 nanometer rms resolution below 5 Hz, and a large measurement range (± 1 mm) to accommodate the initially large segment misalignments. A laser optical system, not described, is used for initial calibration and system alignment. In future works, this system will also be useful for optical scoring.

Actuation: The actuators have been specially designed at Lockheed [1] to meet the strict resolution, dynamic range, smoothness of operation and bandwidth requirements for precision control of segmented optics. When driven in force mode, their bandwidth is 140 Hz. Each actuator is instrumented with an automatic system providing force offloading to reduce power dissipation.

Colocated sensing: Each segment alignment actuator is instrumented with a colocated Kaman inductance position sensor. Each sensor has a 60 nanometer rms resolution below 5 Hz, and a measurement range of $\pm$ 1 mm.

Truss structure: The structure was designed and optimized to emulate a large telescope structure while being able to support the mirror segments in a 1-g environment. Its modal distribution contains several dense clusters and is fundamentally different from the well-spaced distribution of beamlike structures.

*See following page for an actual photograph of the ASCIE Test Bed.

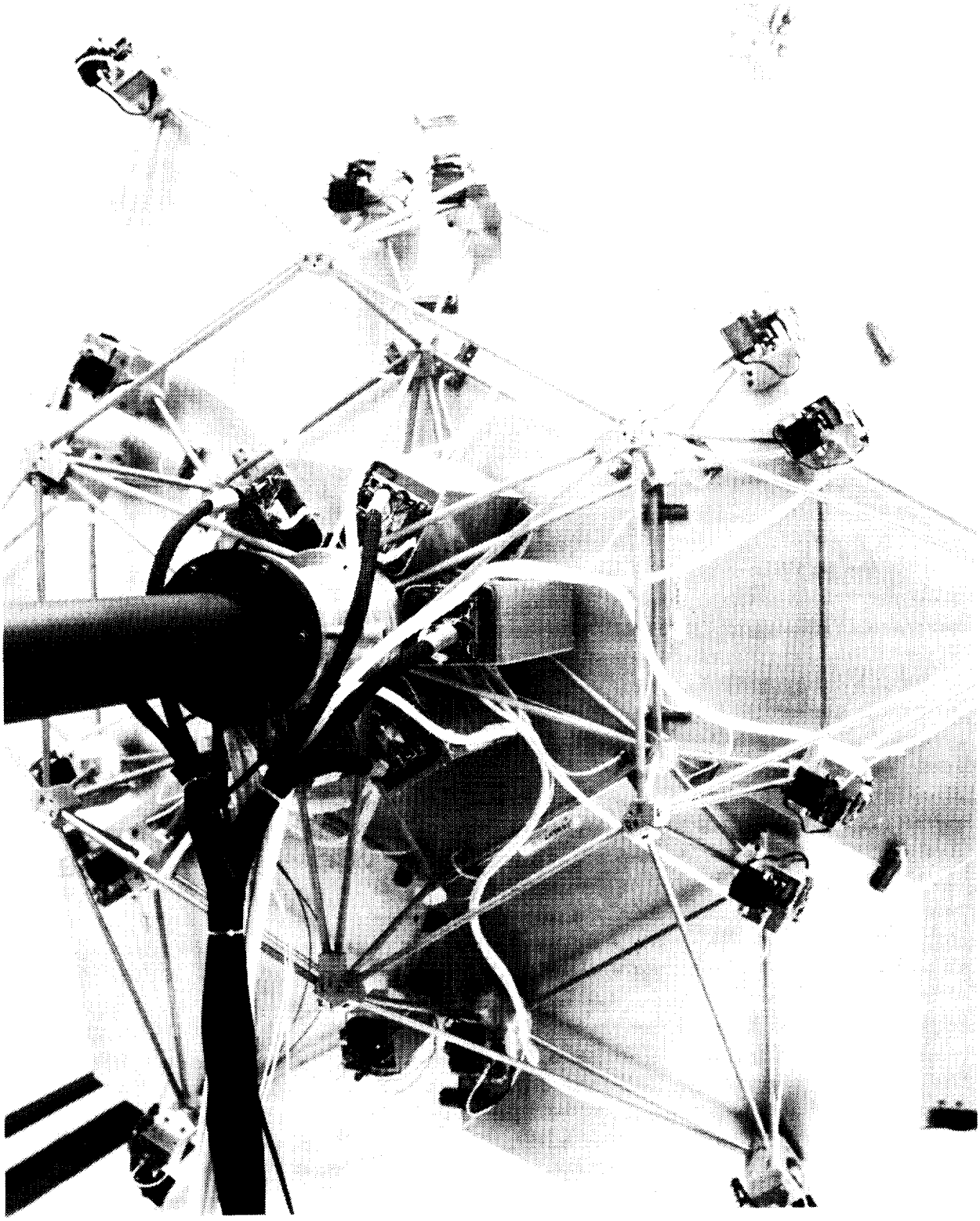

ASCIE Test Bed

Real-time processing and data acquisiton: The ASCIE computer and graphic set up includes an Array Processor, a mini computer, two PCs, and an input/output unit. The Array Processor is an AP-120B, a 12 MFlops machine with 64K of internal memory from Floating Point Systems, fully programmable from the Harris-800 mini computer. The Array Processor is the main computational unit and it is responsible for real-time control processing, signal generation, and real-time Direct Memory Access data transfers to a 256 Kbytes internal memory block residing on the Harris-800 mini computer. The Harris-800 and the PCs are used to monitor the ASCIE experiments via graphical displays of the Kaman sensor readings, the actuator commands, and the mirror segment piston and tilt misalignments. The input/output unit is composed of 32 16-bit analog to digital and 18 16-bit digital to analog converters.

3 CHOICE OF AN EXCITATION TECHNIQUE

System identification can be divided in two phases: a data acquisition phase and an analysis phase. The acquisition phase is particularly important because the quality of the test data determines the quality of the identified model. Good data acquisition requires exciting all of the dynamics of the test article and maintaining good signal to noise ratio via an appropriate choice of the excitation signals. Commonly used excitation signals include impulses, random, and sinusoidal signals. Few impulses or wide-band random excitations are needed to characterize the dynamics of a test article because the response of a system to such excitations is rich in dynamic information. In contrast, many sinusoidal excitations are needed to completely characterize a test article because sinusoidal test signals yield dynamic information at the test frequency only.

Impulse and random excitations allow fast testing, but in practice good signal to noise ratios can be difficult or impossible to achieve with them. Good signal to noise ratio in system identification means that the system response to the excitation is much larger than the system response to the natural disturbances in the whole test frequency range and in all the output dimensions. To ensure good signal to noise ratio, the magnitude of impulse excitations needed to test a complex structure like ASCIE would be destructive. Random excitations offer some more flexibility because filters can be used to concentrate or reduce the energy of the excitation in any desired frequency range. However the magnitude of the response of a multiple-input multiple-output lightly damped system can be quite different depending on the output dimension considered. Consequently if one attempts to maintain good signal to noise ratio in all output dimensions using shaped random signals in some frequency range containing resonant frequencies one may end up resonating the system excessively. Of course, filters could be found to properly shape the excitation in all the input dimensions. This could only be achieved through an iterative testing procedure, because the design of the filters then requires the a priori knowledge of the model of the test article to be found which is impractical.

In contrast, using sinusoidal excitations, it takes much more time to test a system, but it is relatively easy to maintain a given signal to noise ratio and yet ensure non-destructive testing because sinusoidal signals act at a single frequency and in a single input dimension at a time. For this work, we therefore opted for sinusoidal excitations. The complete data acquisition procedure followed for ASCIE is detailed in the data acquisition section, 6.3. The remaining of this section explains how we implemented sinusoidal testing at a given frequency and for a given input direction:

- Two digital sine waves of the same frequency and 90 degrees out of phase are generated by

the Array Processor (AP) and used to construct 18 digital sine waves of the same frequency and different amplitudes and phases.

$$u(n) = uc * cos(2 * \pi * n * of/sf) + us * sin(2 * \pi * n * of/sf)$$

n is the normalized time, $u(n)$ is a vector of size 18, u is the vector sequence of the 18 digital sine waves, π is the number pi = 3.14159..., of is the test frequency, sf is the sampling frequency, uc and us are two constant vectors of size 18 used to vary the amplitudes and phases of the 18 sine waves.

- The 18 digital sine waves are converted into 18 analog signals using 18 digital to analog converters (a2ds). The resulting 18 analog signals are used to command simultaneously the 18 ASCIE segment alignment actuators.

- The 24 analog edge sensor measurements (or the 18 colocated sensor measurements) are converted into 24 (resp. 18) digital signals using 24 (resp. 18) analog to digital converters (d2as) and recorded in real time. The digital signals are then analyzed to extract the coherent (in phase) and the quadrature (out of phase) responses of the ASCIE system to the sinusoidal excitation u. During the analysis, the biases and the harmonic components of the vector response are also extracted.

$$y(n) = yc * cos(2 * \pi * n * of/sf) + ys * sin(2 * \pi * n * of/sf)$$

n is the normalized time, $y(n)$ is a vector of size 24 (resp. 18), y is the vector sequence of the 24 (resp. 18) fundamental digital sine wave responses, yc is the constant vector of size 24 (resp. 18) of the coherent responses, ys is the constant vector of size 24 (resp. 18) of the quadrature responses, of is the oscillator frequency of the sine excitation, sf is the sampling frequency.

4 CHOICE OF AN OPTIMIZATION CRITERION

System identification from measured frequency responses involves fitting the parameterized transfer function matrix of a theoretical linear time invariant system to a measured transfer function matrix at selected frequencies. A criterion is needed to quantify the error between the theoretical and the measured responses at the test frequencies. Most criteria quantify either the average or the peak of the absolute or relative error. To guide our choice, we first discuss the nature of the errors to be expected when dealing with a system like ASCIE.

4.1 Nature of the errors to be expected

We shall classify the identification errors in two categories: stochastic errors, and systematic errors.

Stochastic errors reflect our inability to access the true behavior of the system being tested. Sensor noise, seismic disturbances, laboratory air turbulence, laboratory temperature changes, and measurement unrepeatability for example contribute to these errors in the ASCIE experiments. Long term variations also contribute in the ASCIE experiment since the testing lasted several weeks. The magnitude of these errors can be reduced to a negligible part of the response by careful

experimentation (e.g. vibration isolation, temperature controlled chambers, thermally stabilized electronics) and by careful data acquisition (e.g. averaging to improve repeatability, filtering to reduce the effect of sensor noise and stochastic disturbances).

Systematic errors reflect our inability to capture the true behavior of the system being tested using "reasonable size" linear systems. System nonlinearities are the main source of these errors. As we shall discuss below, the choice of a criterion in the ASCIE experiment is driven by the systematic errors which can be large and highly structured.

To test the ASCIE linearity, the non colocated frequency response of the ASCIE primary mirror and support structure between 15 and 18 Hz was measured for two different amplitudes of the test signals. In the first measurement, the overall amplitude of the segment alignment force excitation was set to give a constant 50 μm root mean squares measured edge sensor response throughout the frequency sweep. In the second measurement, the overall amplitude of the force excitation was set to give a constant 100 μm root mean squares response. The amplitude of the excitation was therefore approximately twice that of the first measurement. Figure (1) and Figure (2) show the principal gains of the two measured transfer function matrices versus frequency.

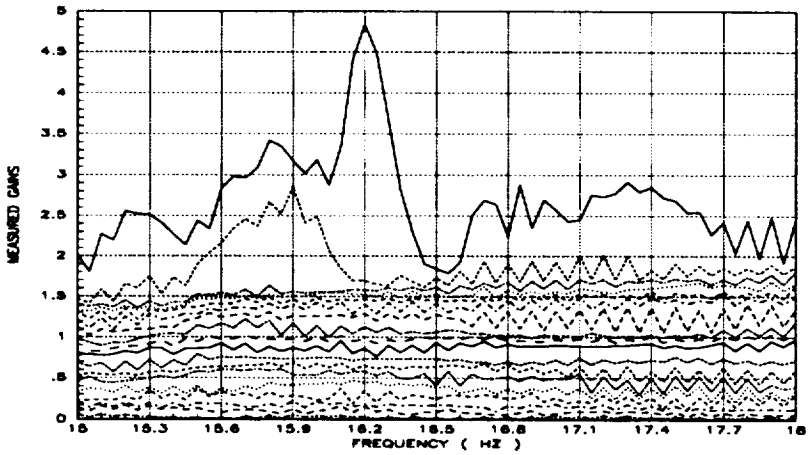

Figure 1: Measured non colocated frequency response of ASCIE for low amplitude test signals

Table (1) contains the dynamic parameters of the two 4-mode-models (Figure (3), and (4)) fitted to the measured frequency responses. It shows about 1% variation in the modal frequencies and up to 50% variation in the modal dampings between the two measurements. The ASCIE response therefore depends highly on the amplitude of the test signals which is typical of nonlinearities. No matter how good the measurements are, the fit errors will remain large because of these nonlinearities.

To illustrate, now a posteriori, the kind of fit error to be expected in the ASCIE identification experiment, we have taken the 50 mode colocated ASCIE identified model (Figure (9)), and perturbed randomly its modal frequencies by 1% or less, and its modal dampings by 10% or less. We then plotted the gains of the absolute error (Figure (5)) and of the relative error (Figure (6)) thus generated. The errors are relatively large. They are representative of what can be expected by fitting a linear model to the measured response of a system which exhibits significant nonlinearities.

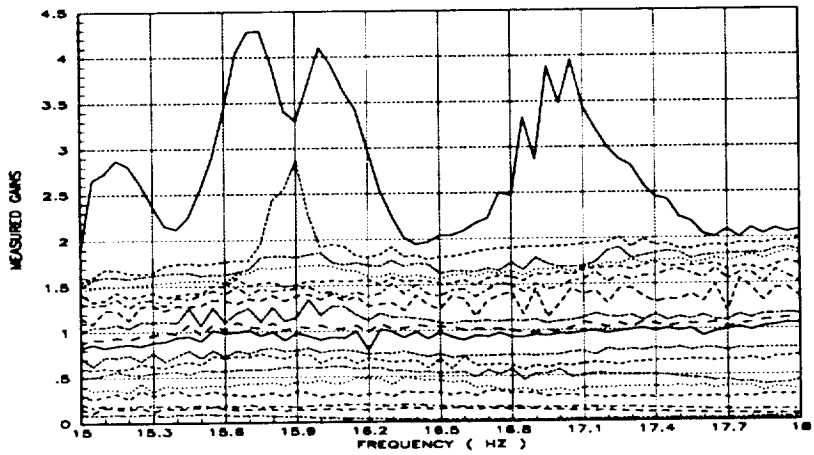

Figure 2: Measured non colocated frequency response of ASCIE for high amplitude test signals

	LOW AMPLITUDE TEST SIGNAL		HIGH AMPLITUDE TEST SIGNAL	
MODE NUMBER	DAMPING %	FREQUENCY (HZ)	DAMPING (increase %) %	FREQUENCY (increase %) (HZ)
1	2.26	15.16	1.91 (-16 %)	15.03 (-0.9 %)
2	1.71	15.81	0.94 (-45 %)	15.73 (-0.5 %)
3	0.78	16.20	1.01 (+29 %)	16.04 (-0.9 %)
4	3.51	17.38	1.65 (-53 %)	17.09 (-1.6 %)

Table 1: Measured modal parameters for two different amplitude test signals

For instance, Figure (5) should be compared to Figure (21) which shows the actual absolute error between the calculated and the measured ASCIE colocated frequency response.

The above observations have far reaching consequences. Most shift invariant identification techniques are based on the premise that the underlying system to be identified is linear. All the errors according to these techniques are treated as measurement errors. This premise is false in the ASCIE experiment and we would like to emphasize further the fundamental differences between measurement and systematic errors. Experimentally, it is possible to quantify how good the measurements are. For instance, bounds and variances of the measurement errors can be estimated, and used a priori in an identification algorithm. Deviations from linearity in contrast cannot be treated as measurement errors because they cannot be quantified a priori without being very conservative. For instance, according to Figure (5) an overall bound on the identification error would be 4 (the peak response of the system is about 8). Non conservative error bounds in this case are highly structured. Constructing such bounds would require the a priori knowledge of the

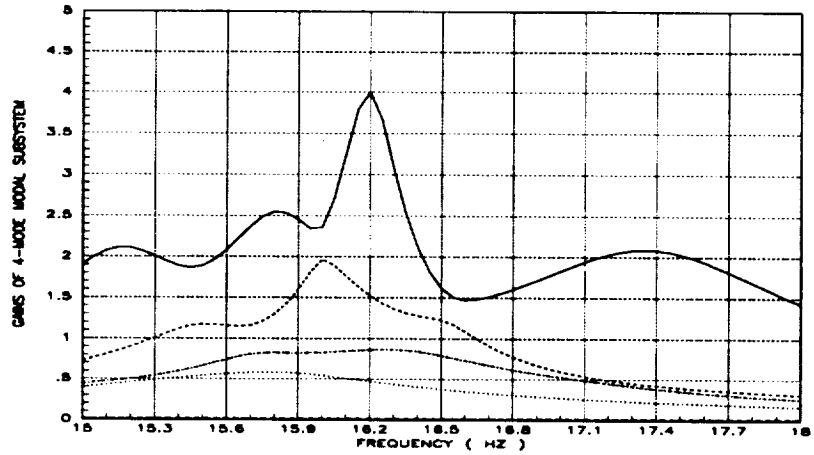

Figure 3: Calculated non colocated modal frequency response of ASCIE for low amplitude segment alignment input forces

model to be found which of course is impractical.

4.2 Relative versus absolute error

Criteria based on the relative error require that the number of measured responses be equal to the number of input forces. When this is not the case, the measurements or the input forces must be constrained, or generalized inverses must be used. For instance, for ASCIE in its non colocated configuration, a geometric transformation could be used to map the 24 edge sensor measurements into 6 piston, 6 petal, and 6 twist motions of the outer mirror segments thus making the number of outputs and the number of inputs equal. However, because the folding motion of the outer mirror segments produces small relative displacements of the mirror segments at the sensor locations, the non colocated ASCIE system is ill-conditioned (the condition number of the static transformation is about 40). Relative error criteria would not appropriately quantify the fit errors in this case because relatively small measurement errors could make the measured frequency response singular and produce large relative errors. In general, relative error criteria are inappropriate for identification of ill-conditioned systems from noisy data. Even when the system is not statically ill-conditioned, ill-conditioning may still appear near the zeros of the system leading again to the problems mentioned above. We shall therefore only consider criteria based on the absolute error for this work.

4.3 Average versus peak errors

The ASCIE segmented optics and support structure exhibit significant nonlinearities. As discussed above, non conservative bounds on the identification errors cannot be developed a priori in this case, so H_∞ peak-error-based identification techniques cannot be used. Figure (5) and Figure (6) show that this is the case whether absolute or relative errors are considered.

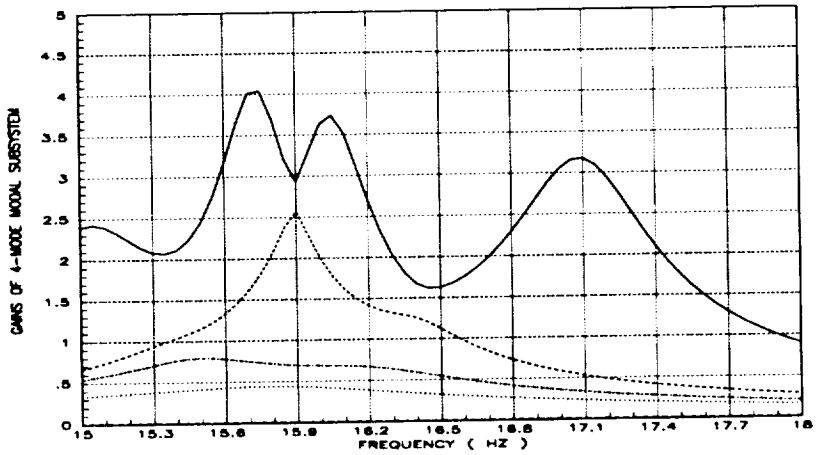

Figure 4: Calculated non colocated modal frequency response of ASCIE for high amplitude segment alignment input forces

Average-based identification techniques such as least-squares, in contrast, do not require any a priori error information: they correlate the measured data at the test frequencies to minimize an average of the modeling errors. As opposed to H_∞ methods, they do not guarantee any bound on the identification error; however, such a bound can always be found a posteriori. For the reasons exposed above, but also because its cost function is easy to compute, and relatively easy to optimize which is critical when dealing with large complex systems like ASCIE, least-squares identification will be used in this work.

Let $H(s)$ be the parameterized transfer function matrix of a theoretical system (s is the usual Laplace variable), let $H_1, \ldots, H_n$ be the ASCIE measured frequency responses at the test frequencies $j\omega_1, \ldots, j\omega_n$, respectively, the least-squares criterion J_0 is:

$$J_0(H) = \sum_{i=1}^{n} Trace\left[(H_i - H(j\omega_i))^*(H_i - H(j\omega_i))\right] \tag{1}$$

4.4 Overview of optimization strategy

The optimization of J_0 over the set of linear transfer function matrices is a difficult nonlinear optimization problem. About 50 modes are needed to model the dynamics of the ASCIE segmented optics and support structure up to 50 Hz. For the colocated identification problem, J_0 therefore depends on approximately 1900 modal parameters. Brute force optimization methods would require an excessive amount of computer time and would most certainly fail to converge if they were not started near a minimum. The proposed optimization strategy is a classical two step initialization-optimization. However, because of the complexity of the present identification problem, a lot of effort is put into the initialization procedure.

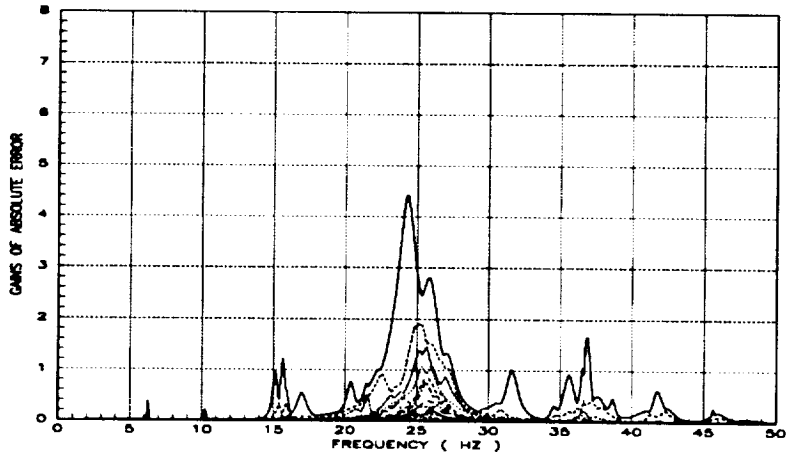

Figure 5: Absolute error generated by perturbing the modal parameters of the 50 mode colocated ASCIE identified model

4.4.1 Initialization procedure

The initialization attempts to find good estimates of the system modal characteristics, if possible, close to the global minimum of J_0. New algorithms are developed to this effect. Some of these algorithms give lower bounds on J_0 that can be used to test the proximity of the global minimum (the lower bounds are tight in the sense that if, for some theoretical model, the theoretical and the measured responses are identical, then the lower bound is achieved).

4.4.2 Optimization procedure

The optimization attempts, starting from the modal parameters estimated in the first step, to reach a minimum. An explicit 2nd order parameter subset optimization method is applied to this effect instead of standard global optimization methods which are computationally too intensive.

5 MODAL DESCRIPTION OF STRUCTURAL SYSTEMS AND MODAL TESTING

The small motions of a structure are best described by a set of partial differential equations. However because it is difficult to derive such a set of equations from physical principles, and because such a set of equations is difficult to use anyway, the dynamics of a structure are often described by a set of equations that describes the motion of the structure at a finite number of selected points called nodes. Such a set of equations is given by:

$$M\,\ddot{z} + L\,\dot{z} + K\,z = f \tag{2}$$

where M is the mass matrix, K is the stiffness matrix, L is the damping matrix, z is the vector of the displacements at the selected nodes, and f is the vector of the forces applied at the selected

C-4

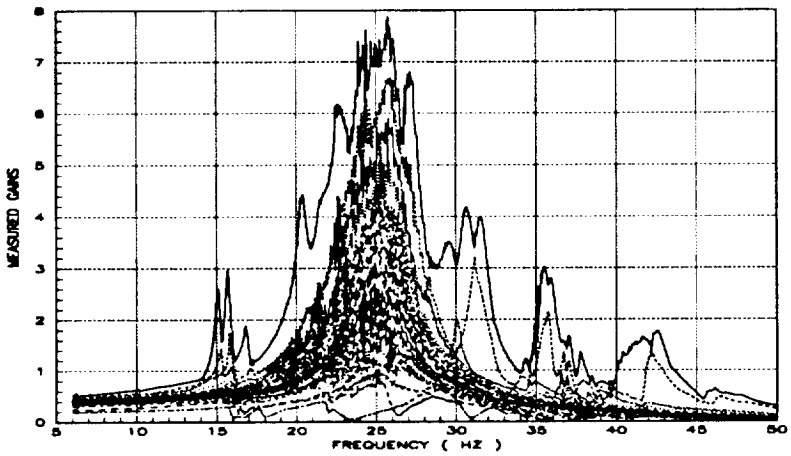

Figure 6: Relative error generated by perturbing the modal parameters of the 50 mode colocated ASCIE identified model

nodes. M and K are positive definite matrices. They can be constructed, using Finite Element Analysis, from the geometric and material properties of all the structural elements that make the system. In contrast, for most structures, analytical methods alone fail to construct the matrix L. L need not be symmetric. Very often, L is assumed to be relatively small, and in most Finite Element Analyses it is set to 0. The force vector f is typically composed of known (or control) forces u, and unknown environmental disturbance forces d. Control forces apply to only some of the nodes, so that the force vector can be rewritten:

$$f = E\,u + d \tag{3}$$

E is the control distribution matrix.

The displacements, the velocities, or the accelerations at some selected nodes may be measured. When only the displacements at some of the nodes are measured, the measurement equation is:

$$y = S\,z + e \tag{4}$$

S is the sensor distribution matrix. e is the measurement error vector.

5.1 Modal description and modal testing of structures with proportional damping

Under the proportional damping assumption, L is a linear combination of M and K. This assumption is often made for convenience, not on physical ground. The dynamic equations of the structure (2) can then equivalently be described by a set of dynamically uncoupled 2nd order ordinary scalar differential equations. Each of these equations describes what is called a natural structural mode. Such a set of equations is obtained using the modal transformation:

$$z = \Phi q \tag{5}$$

such that

$$\Phi^T M \Phi = I \tag{6}$$

$$\Phi^T K \Phi = \Omega^2 \tag{7}$$

where I is the identity matrix, and where Ω is the diagonal matrix of the modal frequencies. The columns of Φ are the mode shapes, and q is the vector of the modal coordinates. Under the proportional damping assumption, the matrices M, L, and K can be simultaneously diagonalized, so that we can also write:

$$\Phi^T L \Phi = 2 \xi \Omega \tag{8}$$

where ξ is the diagonal matrix of the modal dampings (or damping ratios).

The dynamic equations of the structure can then be rewritten:

$$\begin{cases} \ddot{q} + 2 \xi \Omega \dot{q} + \Omega^2 q = B_2 u + \Phi^T d \\ y = C_1 q + e \end{cases} \tag{9}$$

where we have defined $B_2 = \Phi^T E$ and $C_1 = S \Phi$. According to these definitions, the rows of B_2 are the mode shapes at the actuator locations, and the columns of C_1 are the mode shapes at the sensor locations.

5.1.1 Spectral description of structures with proportional damping

According to (9), the transfer function matrix from actuator commands to sensor measurements is:

$$H(s) = C_1(s^2 I + 2 \xi \Omega s + \Omega^2)^{-1} B_2 \tag{10}$$

5.1.2 Modal testing of structures with proportional damping

When the proportional damping assumption is satisfied, if one had an actuator at each of the structural nodes ($E = I$), one could excite each structural mode separately. For instance, to excite only the first mode, one would set $u = M \Phi_1 u_1$ where Φ_1 is the first column of the modal matrix Φ. When actuators are available at only some nodes, the best that can be done to excite a mode is to maximize the projection of the actuator force vector on the corresponding mode shape at the actuator location. Similarly, when the proportional damping assumption is satisfied, if one had a position sensor at each of the nodes (S=I), one could observe selectively each structural mode of the system. For instance, to observe only the first mode, one would form the linear combination of the measurements $q = \Phi_1^T M y$ where again Φ_1 is the first column of Φ. In general, this is not possible if sensors are available at only some nodes on the structure. In actual hardware however one would really need infinitely many actuators to excite a pure mode, and infinitely many sensors to observe a pure modal response, because the columns of the modal matrix Φ only interpolate the physical mode shapes of the real system at the nodes.

Modal testing involves using the actuators simultaneously to excite the structure and the sensors simultaneously to measure the structural response to isolate each mode of the structure and measure its characteristics. In practice, it is difficult to carry out because of the limited number of actuators

and sensors, and because the proportional damping assumption may be violated. Structural test engineers circumvent the first limitation by using many shakers and many accelerometers. This procedure is invasive because the extra hardware modifies the mass and inertia properties of the article being tested. The second limitation is not critical for very lightly damped structures.

Assuming that the mode shapes at the sensor and at the actuator locations are orthogonal, then testing pure modal response in actual hardware is easy because if a pure mode is being excited at a resonant frequency, the various displacements at the sensor locations are all in phase with respect to each other, and in quadrature with respect to the excitation. These properties form the theoretical basis for many current modal testing methods.

5.2 Modal description and modal testing of structures with nonproportional damping

When the proportional damping assumption is violated, it is still possible to find a set of dynamically uncoupled 2nd order ordinary scalar differential equations to describe the system. The non proportional damping allows a transfer of energy between modes. Consequently, a combination of force and rate control is needed to excite a pure mode, and similarly a combination of position and rate measurements is needed to observe a pure mode. From these physical considerations alone, the modal equations of a linear system with non proportional damping, assuming that such equations exist at all, must therefore have the following form:

$$\begin{cases} \ddot{q} + 2\,\xi\,\Omega\,\dot{q} + \Omega^2 q = B_1\dot{u} + B_2 u + B_{d1}\dot{d} + B_{d2} d \\ y = C_1 q + C_2 \dot{q} + D\,u + D_d d + e \end{cases} \tag{11}$$

where q is the vector of the modal coordinates, Ω is the diagonal matrix of the modal frequencies, and ξ is the diagonal matrix of the damping ratios. The distribution matrices involved in the above set of equations are not all independent. For instance, if these equations model a system with force command and position measurements then the following constraints must hold:

$$\begin{cases} D = -C_2 B_1 \\ D_d = -C_2 B_{d1} \\ C_1 B_1 + C_2(B_2 - 2\xi\Omega B_1) = 0 \\ C_1 B_{d1} + C_2(B_{d2} - 2\xi\Omega B_{d1}) = 0 \end{cases} \tag{12}$$

It is shown in Appendix C that the dynamic equations of a system with nonproportional damping, force commands, and position measurements can indeed equivalently be rewritten in the modal form postulated above.

5.2.1 Spectral description of structures with non proportional damping

According to (11),(12), the transfer function matrix of a structural system with non proportional damping, force commands, and position measurements is:

$$H(s) = (C_1 + s\,C_2)(s^2 I + 2\,\xi\Omega\,s + \Omega^2)^{-1}(s\,B_1 + B_2) - C_2 B_1 \tag{13}$$

where $C_1 B_1 + C_2(B_2 - 2\xi\Omega B_1) = 0$.

5.2.2 Modal testing of structures with non proportional damping

For a structure with non proportional damping, a combination of force and rate command is needed to excite a pure mode, and a combination of position and rate measurements is needed to observe a pure modal response. For a structure with non proportional damping, when a pure mode is being excited at a resonant frequency, the various displacements at the sensor locations are not in phase with respect to each other, and not in quadrature with respect to the excitation. It is therefore difficult to experimentally isolate the modes of a structure with non proportional damping to measure their modal characteristics. Standard vector force excitation, and standard tests for modal response purity fail in this case.

5.3 Reduced order modal description of structural systems

Infinitely many modes are needed to exactly describe the dynamic of a flexible structure. Only the lowest frequency modes however are needed in practice. One convenient way to model the effect of the "high" frequency modes at low frequencies is to assume that their response is quasi-steady, which is equivalent to recover static fidelity. For instance, consider the modal expansion of the transfer function matrix of a system with proportional damping:

$$H_\infty(s) = \sum_{i=1}^{\infty} \frac{c_i b_i}{s^2 + 2\xi_i\omega_i s + \omega_i^2} \tag{14}$$

Keeping the first n modes and assuming that the response of the other modes is quasi-steady, an approximation of H_∞ at low frequencies (say below ω_n) is:

$$H(s) = \sum_{i=1}^{n} \frac{c_i b_i}{s^2 + 2\xi_i\omega_i s + \omega_i^2} + \sum_{i=n+1}^{\infty} \frac{c_i b_i}{\omega_i^2} \tag{15}$$

or in matrix form with the obvious definitions:

$$H(s) = C(s^2 I + 2\,\xi\Omega\, s + \Omega^2)^{-1} B + D \tag{16}$$

5.4 Spectral descriptions used in this work

Two spectral descriptions will be used in the ASCIE identification. Both of them can account for non proportional damping.

The first description is closest to the physical system:

$$H(s) = C(M\, s^2 + L\, s + K)^{-1} B + D \tag{17}$$

C is then the sensor distribution matrix, B is the control distribution matrix, and D accounts for the contribution of the unmodeled modes at low frequencies. M, L, and K can be viewed as the mass, damping, and stiffness of the system respectively seen at the actuator and at the sensor locations.

The second description is a modal description:

$$H(s) = (C_1 + s\, C_2)(s^2 I + 2\,\xi\Omega\, s + \Omega^2)^{-1}(s\, B_1 + B_2) + D \tag{18}$$

with the physical constraint $C_1B_1 + C_2(B_2 - 2\xi\Omega B_1) = 0$. This last description will be used for parameter optimization. No attempt however will be made to enforce the physical constraint which arises because only force commands and position measurements are used in the ASCIE experiment. This is not a serious shortcoming because any good model approximation to the physical system will tend to satisfy this constraint.

6 NEW ON-LINE MODAL TUNING, DATA ACQUISITION, AND EXPERIMENTAL RESULTS

On-line modal testing is useful for limited modal surveys. It was first proposed by Lewis and Wrisley [14]. Current on-line modal testing techniques were established in the late 70's early 80's [7]. The excitation technique closest to the one used in this work is called modal dwell. It requires tuning the polarities and the relative amplitudes at one frequency of several shakers located at discrete points on the structure to produce a pure modal response. Several methods, such the "amplitude-weighted sum of quadrature peaks" and the Asher [8] or Ibanez [15] determinant techniques, were developed to detect the presence of a mode and determine the force distribution to produce tuned modal responses. They assume that the response and the excitation, at a resonant frequency, are in quadrature. Delays, ill-conditioning of the type encountered with ASCIE in its non-colocated configuration, high modal density that alters the purity of the modal responses, all make these methods unreliable for testing complex systems.

Classical modal testing of large systems is costly. It requires a lot of instrumentation, cabling, and expensive data acquisition systems. Even though tuning techniques have been automated [16], they can still require a prohibitive testing time. This time is typically larger than the time required to measure the full frequency dependent system admittance matrix. The time to test complex flexible structures is therefore better spent measuring admittance matrices which have "all" the information about the system response. This relieves one from the requirement of exact tuning. Modal parameters are then obtained off-line by processing the measured spectral data, not experimentally. In testing ASCIE, the control hardware was used. No special purpose instrumentation was added, a situation similar to on-orbit testing of a spacecraft.

6.1 New on-line modal tuning technique

In view of the above limitations, new tuning techniques must be developed for modal tuning to become useful in practice. The approximate modal tuning objective used for ASCIE was to maximize the root mean squares displacement for a given root mean squares force excitation. This objective is the generalization of the single-input single-output force-displacement gain concept to the case of multiple excitation forces and multiple measured responses. At each frequency, to maximize this force-displacement gain, the relative magnitudes and the relative phases of the various sinusoidal forces applied to the test article must be adjusted. When the maximum is achieved, the corresponding normalized (unit) complex force vector is called a *major principal force vector*, the corresponding normalized (unit) complex displacement vector is called a *major principal displacement vector* at the test frequency.

Classical modal tuning (or modal dwell) techniques can be difficult to implement. Experimental factors such as number of excitations, number of responses, measurements non colocated with the

excitations, delays, non-proportional damping, lack of orthogonality of the mode shapes in high modal density regions, and ill-conditioning affect it or make it fail. In contrast, it is always very easy to tune the force vector to the maximum displacement/force gain at a given frequency. One way to do that is to measure the complex admittance matrix of the system at this frequency and compute its singular value decomposition [17]. The physical and the analytical data are then related as follows: the maximum singular value of the admittance matrix is the maximum displacement/force gain of the system; the corresponding right (input) singular vector of the admittance matrix is a major principal force vector; the corresponding left (output) singular vector of the admittance matrix is a major principal displacement vector.

For lightly damped structures, gain tuning and modal dwell are very closely related. Consider for example the modal expansion of the transfer function matrix of a lightly damped structure with proportional damping:

$$H(s) = \sum_{i=1}^{n} g_i \frac{c_i b_i}{s^2 + 2\xi_i \omega_i s + \omega_i^2} \tag{19}$$

where the c_i's and the b_i's are the normalized mode shapes at the sensor and the actuator locations, respectively, and the g_i's are scalars. At the resonant frequency ω_i, the response of the system will usually be dominated by the modal response of mode i:

$$H(j\omega_i) \sim g_i \frac{c_i b_i}{2\xi_i \omega_i^2} \tag{20}$$

which shows that the maximum gain of the system at the frequency ω_i is nearly $\sigma_i = \frac{g_i}{2\xi_i \omega_i^2}$, that a major principal force vector is nearly b_i that is the mode shape at the actuator locations, and that a major principal displacement vector is nearly c_i that is the mode shape at the sensor locations. The singular value decomposition of $H(j\omega_i)$ in this case is also approximately:

$$H(j\omega_i) \sim \sigma_i c_i b_i \tag{21}$$

Gain and modal tuning are therefore nearly equivalent. The former however has the significant advantage of being easy to achieve experimentally.

Based on these ideas, it is easy to devise experiments to measure the modal parameters of some mode. First perform a frequency sweep to measure the force-displacement system admittance matrix in some frequency range around the resonant frequency of the target mode. Then find analytically the maximum gain of the system in this frequency range by singular value analysis of the measured frequency response. The frequency where the maximum gain reaches its peak is the resonant frequency ω_i of the target mode, the right singular vector b_i^T of the admittance matrix at the frequency ω_i is the mode shape at the actuator locations, and the left singular vector c_i of the admittance matrix at the resonant frequency ω_i is the mode shape at the sensor locations. If the singular vectors c_i and b_i are not real, then they can be replaced by real vectors whose product best approximates $c_i b_i$. Once the mode shapes b_i^T and c_i are available, a new frequency sweep can be performed where the polarities and the relative magnitudes of the various forces are adjusted according to b_i^T and where a linear combination of all the responses is formed according to c_i. This sweep is analogous to a single-force-excitation single-response-measurement sweep and all the standard experimental techniques to test modal purity, and measure the resonant frequency and the modal damping of the target mode apply. For instance, phase displays can be used to test

modal purity and find the resonant frequency, and free decay from a forced response can be used to measure the modal damping.

6.2 Experimental demonstration of new on-line modal tuning technique

To illustrate the effectiveness of the experimental procedure described in the previous section, the non-colocated admittance matrix of the ASCIE segmented optics and support structure was measured between 22 and 33 Hz (Figure 7).

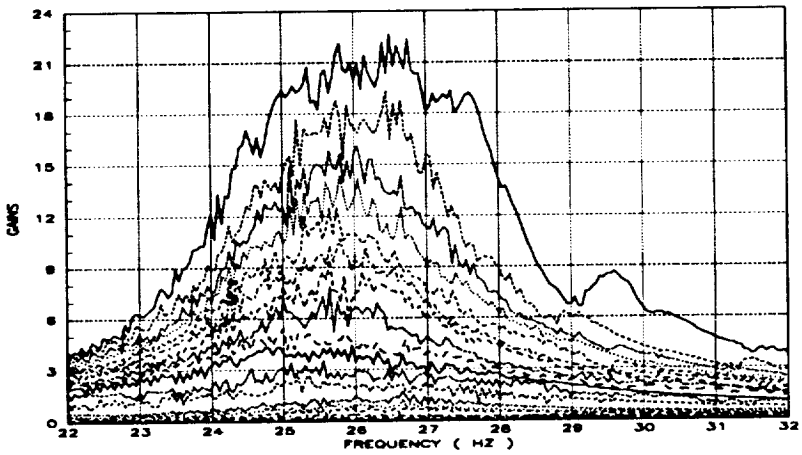

Figure 7: ASCIE non colocated frequency response in high modal density region

The singular value decomposition of the admittance matrix at 27 Hz was then computed to determine the mode shapes at the actuator and sensor locations of the dominant mode around this frequency (note that the resonant frequency does not need to be known exactly). A single-input single-output sweep using this mode shape information as described in the previous section was then performed.

(Figure 8) shows the measured modal response. The phase plot shows that the phase drops by 180 degrees as the sweep goes through the resonant frequency as it should for a pure mode response. The modal frequency and the damping ratio, obtained by curve fitting the modal response, are 26.9 Hz and 3.3% respectively.

Unlike current modal dwell techniques, gain tuning does not use any phase information. It is purely based on the dominance of the modal response of the target mode near the resonant frequency. Variations on the gain tuning technique which incorporate phase information are possible but will not be explored here.

Of course, gain tuning will fail to isolate a target mode if its response does not dominate the overall system response near its resonant frequency. This is the case in high modal density regions if the modes have resonant frequencies close to one another, if mode shape orthogonality is only approximately satisfied, and if the target mode has relatively low response. This is not however a limitation specific to gain tuning; current modal dwell techniques would also fail in this case. The fact is that it is in general impossible to experimentally isolate all the modes of a structure to

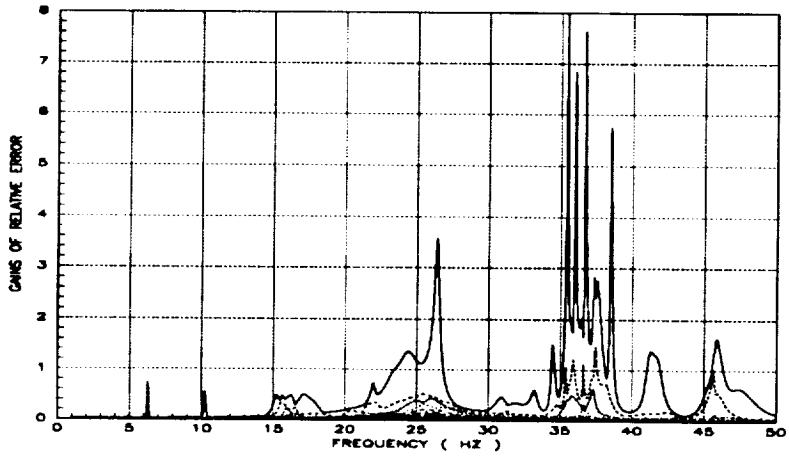

Figure 8: Frequency response of dominant mode around 27 Hz extracted by on-line modal tuning

measure their modal characteristics. Analytical techniques that can determine the modal properties of a structure without having to differentiate the modes must be used.

6.3 New data acquisition technique

In the previous section, we have introduced the concepts of principal gains, principal force vectors, and principal displacement vectors, and illustrated their importance in on-line modal tuning, an area the modal test engineers know well. The same concepts play a central part in the data acquisition procedure described next.

Recognizing the difficulty of getting accurate estimates of all the modal parameters of such a complex system like ASCIE using on-line modal tuning alone, the data acquisition process was focused on acquiring good data that could subsequently be analyzed off-line.

The data acquisition process is a linear, multiple-force-excitation, sinusoidal sweep between 1 and 50 Hz. The sweep dwells every 0.05 Hz. At each frequency, the data acquisition proceeds as follows:

(1)
- A set of 18 estimated orthonormal complex principal force vectors and estimated principal gains are defined. These gains give an estimate of the root mean squares response to a unit force excitation vector whose components are distributed according to the corresponding principal force vectors. The principal force vectors and the principal gains are set arbitrarily at the first test frequency. Subsequently they are updated from one test frequency to the next following a procedure described later.
- Two 90 degree out of phase digital reference sine waves at the test frequency are generated by the AP-120B Array Processor. These sine waves are modulated to produce 18 sinusoidal signals to drive the segment alignment actuators. The relative phases and amplitudes of these 18 sinusoidal signals are set according to the major principal force vector to produce maximum displacement per unit force, and the overall magnitude of

the excitation is set to give a 100 μm root mean squares displacement response. The excitation is then applied.

- The Harris-800 host computer waits for a specified length of time to allow the ASCIE structure to reach a steady state response, and then requests the response data. The reading of the 18 colocated Kaman position sensors (or the 24 non colocated Kaman position edge sensors) are then digitized and recorded in real-time together with the 18 discrete actuator commands in a 256 Kbyte buffer. Once the buffer is filled, the time response data are transferred into the local host computer memory and analyzed. The bias, the fundamental component at the excitation frequency, and a specified number of harmonics are extracted from the recorded signal time-histories. For each signal, a parameter indicative of the quality of the data, the Total Wave Distorsion, is computed. If a signal s is decomposed as:

$$s(t) = b + f(t) + h(t) + n(t) \tag{22}$$

where the scalar b is the bias, the function f is the fundamental component, the function h is the sum of a specified number of harmonics, and the function n is the noise, the Total Wave Distorsion TWD of the signal is defined as:

$$TWD = \frac{\|f\|}{\sqrt{\|h\|^2 + \|n\|^2}} \tag{23}$$

- The spectral data and the Total Wave Distorsion vector are stored in separate arrays.
- The excitation and measurement procedure just described in correspondence with the major principal force vector is repeated for the next principal force vector and so on until all the 18 orthonormal principal force vectors are considered.

(2)
- The transfer function matrix of the system is constructed from the measured spectral data, and its singular value decomposition is computed. The right singular vectors, and the singular values of this decomposition are the principal force vectors, and the principal gains respectively of the system at the test frequency.
- The test frequency, the spectral data, the 18 principal gains, and the matrix of all 18 Total Wave Distorsion vectors are stored on a disk file.

(3) The frequency is incremented and (1) and (2) are repeated. The principal force vectors and the principal gains computed at the last test frequency become the estimated principal force vectors and principal gains at the new test frequency.

The iteration lasts until the whole frequency range between 1 and 50 Hz is covered.

The whole measurement procedure has several important features worth emphasizing:

- For small frequency sweep increments, the principal force vectors will change only slightly from one test frequency to the next. Gain tuning is therefore approximately realized as the data acquisition progresses. According to the previous sections, this in turn means that modal dwell to the dominant modes of the system is also approximately realized as the data

acquisition progresses. The frequency sweep increment could be decreased to achieve modal frequency dwell when sharp increases in the maximum gain of the system are encountered which indicates that the sweep is approaching a resonant frequency, but we did not include this feature in our data acquisition procedure.

- The overall amplitude of the excitation is always set, to the extent possible, to give a prescribed overall displacement response. We have observed, by examining the values taken by the Total Wave Distorsion parameter that the quality of the data acquired this way is better than the quality of the data acquired by driving one actuator at a time. When the number of measured responses equals the number of excitations, the above excitation method could in fact be refined to produce nearly the same amplitude response at all the sensor stations. This uniform excitation method would give very good quality data but we did not implement it.

- The overall amplitude of the excitation is always set, to the extent possible, to give a prescribed overall displacement response. The overall amplitude of the excitation therefore decreases when passing through a resonant frequency. Modal test engineers have observed that this excitation technique reduces the effects of the nonlinearities. We think that this observation must be taken with caution. It is true that this excitation procedure can be used to ensure that the response will not exceed the working range of the instruments at any sensor station, and to ensure that the structure will not be damaged by being resonated excessively. This procedure is in a sense necessary for safe testing and yet maintaining good quality data. A nonlinear structure, however, exhibits different response depending on the amplitude of the excitation; varying the amplitude of the excitation continuously through the sweep might therefore not be the best strategy.

7 OFF-LINE MODAL CHARACTERIZATION, NEW ALGORITHMS AND APPLICATION TO ASCIE

This section describes new analytical techniques to extract the modal characteristics of a test article for its measured frequency response. These techniques are very closely related to the on-line gain-tuning-based-modal-dwell technique developed in the previous section, because they also extract modes on the basis of the dominance of their response in some frequency range around their resonant frequencies. Analytical modal separation is however easier to perform and more powerful than experimental modal dwell: the frequency response of the system is available for analysis over a whole frequency range and not just at the single test frequency; several modes can be extracted simultaneously, when the resonant frequencies are close to one another and the mode shapes are not orthogonal to each other; finally non dominant modes can be extracted from the residual frequency response after the contribution of the dominant modes to the system response has been removed. Like on-line modal dwell, the modal characteristics determined by analytical modal separation are not optimal because their value is based on the response of the system in some frequency range around the resonant frequencies and not on the system overall frequency response. They are nevertheless very useful to start global optimization procedures. The following section details the new algorithms and illustrates their application to the modal identification of

the colocated frequency response of the ASCIE segmented optics and support structure (Figure 9).

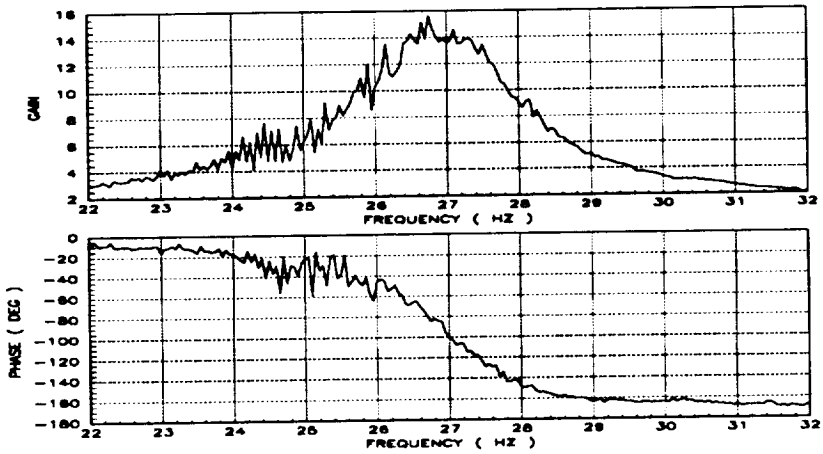

Figure 9: Measured colocated frequency response of ASCIE

7.1 Algorithms for extracting the combined response of several dominant natural modes in a given frequency range

Consider the colocated frequency response of the ASCIE segmented optics and support structure between 13 and 18 Hz (Figure (10)). We want to extract the modal response of the 4 dominant natural modes of ASCIE in this frequency range.

Extracting a single mode response involves determining the proper distribution of excitation forces and the proper linear combination of the measured responses (that is the mode shapes at the actuator and the sensor locations respectively) as in on-line modal dwell. Similarly, extracting a multiple mode response involves determining several distributions of excitation forces and several linear combinations of the measured responses. The distributions of excitation forces in this later case could be the mode shapes at the actuator locations, but they need not be. Independent linear combinations of the mode shapes are also perfectly appropriate. This fact is captured in the mathematical concept of range, that is the space spanned by multiple vectors. Accordingly, we shall call *modal spaces* the spaces spanned by the mode shapes of multiple modes at the actuator or the sensor locations. Thus modal spaces can equivalently be described by any maximum set of independent linear combinations of the mode shapes.

Let the theoretical frequency response of the ASCIE modal subsystem between 13 and 18 Hz be:

$$H(s) = C\,(M\,s^2 + L\,s + K)^{-1}B + D \tag{24}$$

where:

- the columns of C are independent linear combinations of the mode shapes at the sensor locations.

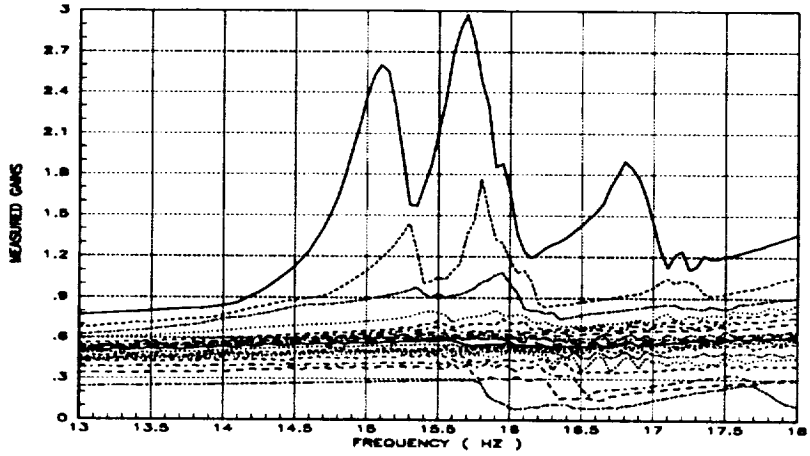

Figure 10: Measured ASCIE colocated frequency response between 13 and 18 Hz

- the rows of B are independent linear combinations of the mode shapes at the actuator locations.
- D accounts for the effects of the modes outside of the frequency range being analyzed.
- M, L, and K can be viewed as mass, damping, and stiffness matrices, respectively.

Without loss of generality, we shall assume that B and C are orthogonal matrices, that is $C^T C = I$ and $B\ B^T = I$.

Let $H_1, \ldots, H_n$ be the ASCIE measured frequency responses, and let $\Delta_1, \ldots, \Delta_n$ be the differences between the measured and the theoretical responses at the frequencies $j\omega_1, \ldots, j\omega_n$ respectively. The least-squares curve fitting problem would be to find the real matrices C, B, D, M, L, and K such that:

$$J(C, B, D, M, L, K) = \sum_{i=1}^{n} Trace(\Delta_i^* \Delta_i) \tag{25}$$

is minimized.

Instead of solving this problem exactly, which at present nobody knows how to do, we propose solving this problem approximately in three steps. In the first step, we estimate the modal space at the sensor locations by solving exactly a relaxed optimization problem. In the second step, dual of the first step, we estimate the modal space at the actuator locations. In the third step, we determine the modal dynamics.

7.1.1 Estimating the modal spaces at the sensor locations

Let $X_1, \ldots, X_n$ be the state of the theoretical system at the frequencies $j\omega_1, \ldots, j\omega_n$, then:

$$[H_1, \ldots, H_n] = C\,[X_1, \ldots, X_n] + D\,[I, \ldots, I] + [\Delta_1, \ldots, \Delta_n] \tag{26}$$

If $[X_1, \ldots, X_n]$ is allowed to be a general complex matrix X, then the minimization with respect to C, X, and D of

$$\tilde{J}(C, D, X) = \sum_{i=1}^{n} Trace(\Delta_i^* \Delta_i) \tag{27}$$

is equivalent to finding the best biased approximation to the matrix $[Re[H_1, \ldots, H_n], Im[H_1, \ldots, H_n]]$ by a matrix of lower rank. This problem is solved exactly in Appendices A and B and its solution defines uniquely the range of C, that is the estimated modal space at the sensor locations. Of course, since C is based on the dominant part of the frequency response in the frequency range being analyzed, C will be a close approximation to the true modal space of the target modal subsystem at the sensor locations only if the modal frequency response of this subsystem dominates the overall system frequency response.

The optimization problems with criteria J and $\tilde{J}$ are very closely related. If $\tilde{J}^*$ and J^* are the optimal values of J and $\tilde{J}$, respectively, then

$$\tilde{J}^* \leq J^* \tag{28}$$

$\tilde{J}$ is a lower bound for J. Thus if, in the course of minimizing J, values of J close to $\tilde{J}^*$ are obtained, we can be confident that a global minimum of J is being achieved. Furthermore, if, for some theoretical model, the theoretical and the measured frequency responses are identical, then the value of C obtained by minimizing $\tilde{J}$ corresponds to a global minimum of J. Direct optimization of J, in general, would not find a global minimum because J may have multiple minima.

7.1.2 Estimating the modal space at the actuator locations

The modal space at the actuator locations is determined in the dual manner.

7.1.3 Application: non parametric modal frequency response of ASCIE 4-mode-model between 13 and 18 Hz

The algorithm described above were applied to find the modal spaces at the sensor and at the actuator locations of a 4-mode model of ASCIE from the measured ASCIE frequency response between 13 and 18 Hz. Using these modal spaces, the "measured" frequency response of the modal subsystem can now be extracted from the measured overall system frequency response. This is done by considering only force distributions that belong to the modal space at the actuator locations, and only linear combinations of the measured responses that belong to the modal space at the sensor locations.

Analytically, if $H_{m1}, \ldots, H_{mn}$ denotes the estimated modal response at the frequencies $j\omega_1, \ldots, j\omega_n$, then:

$$H_{mi} = C^T (H_i - D)\, B^T \qquad i = 1 : n \tag{29}$$

The estimated non parametric frequency response of the 4-mode-subsystem between 13 and 18 Hz is shown in Figure (11). The frequency response of the residual system left after the modal subsystem is removed from the overall system frequency response is shown in Figure (12). This frequency response clearly illustrates that the modal response is well extracted.

To complete the modal identification, we now have to extract the dynamics of the 4-mode-subsystem with 4 inputs, 4 outputs, and with frequency response H_m, a problem much easier to solve than the original one with 18 inputs and 18 outputs.

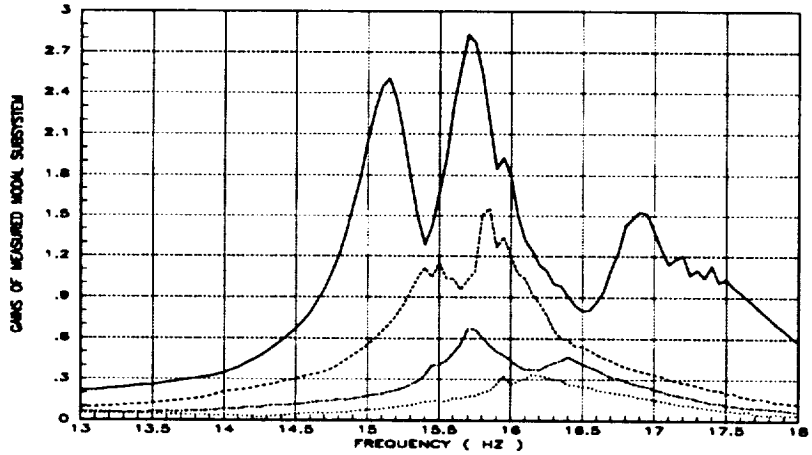

Figure 11: Non parametric frequency response of ASCIE 4-mode-model between 13 and 18 Hz

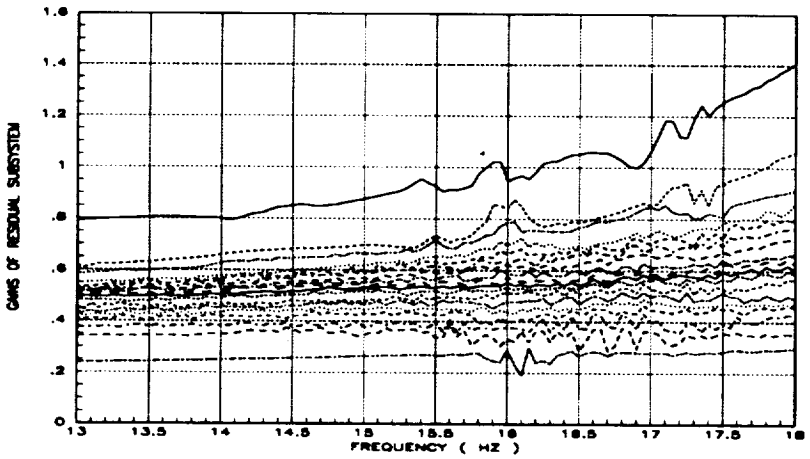

Figure 12: Residual ASCIE frequency response between 13 and 18 Hz after the estimated modal response is removed

7.1.4 Estimating the modal dynamics

Let the theoretical dynamic response of the modal subsystem be:

$$\bar{H}(s) = (M\ s^2 + L\ s + K)^{-1} \tag{30}$$

Let $\Delta_1, \ldots, \Delta_n$ be the difference between the theoretical and the measured modal responses at the frequencies $j\omega_1, \ldots, j\omega_n$ respectively. The least-squares curve fitting problem is to find the real matrices M, L, and K such that:

$$J(M, L, K) = \sum_{i=1}^{n} Trace(\Delta_i^* \Delta_i) \tag{31}$$

is minimized.

As a first step, we propose solving exactly a related linear least-squares problem. We have:

$$\begin{cases} H_{m1} = (M\,(j\omega_1)^2 + L\,(j\omega_1) + K)^{-1} + \Delta_1 \\ \ldots\ldots\ldots\ldots\ldots\ldots\ldots\ldots\ldots\ldots\ldots\ldots\ldots\ldots\ldots\ldots \\ H_{mn} = (M\,(j\omega_n)^2 + L\,(j\omega_n) + K)^{-1} + \Delta_n \end{cases} \tag{32}$$

What is often done [1], is to rewrite this set of equations as:

$$\begin{cases} H_{m1}(M\,(j\omega_1)^2 + L\,(j\omega_1) + K) = I + \Delta_1(M\,(j\omega_1)^2 + L\,(j\omega_1) + K) \\ \ldots\ldots\ldots\ldots\ldots\ldots\ldots\ldots\ldots\ldots\ldots\ldots\ldots\ldots\ldots\ldots\ldots\ldots\ldots\ldots\ldots\ldots \\ H_{mn}(M\,(j\omega_n)^2 + L\,(j\omega_n) + K) = I + \Delta_n(M\,(j\omega_n)^2 + L\,(j\omega_n) + K) \end{cases} \tag{33}$$

which is now a linear set of equations in M, L, and K, and solve the linear least-squares problem with criterion

$$\bar{J}(M, L, K) = \sum_{i=1}^{n} Trace(\bar{\Delta}_i^* \bar{\Delta}_i) \tag{34}$$

where $\bar{\Delta}_i = \Delta_i(M\ j\omega_i{}^2 + L\ j\omega_i + K)$, which is a frequency weighted version of the original least-squares problem. It is our experience that the estimates of M, L, and K obtained that way are usually very poor and cannot be used to start the optimization of the original least-squares problem with criterion J. What we propose instead, is to restore appropriate frequency weighting by rewriting the above set of equations as:

$$\begin{cases} H_{m1}(M\,(j\omega_1)^2 + L\,(j\omega_1) + K)H_{m1} = H_{m1} + \Delta_1(M\,(j\omega_1)^2 + L\,(j\omega_1) + K)H_{m1} \\ \ldots\ldots\ldots\ldots\ldots\ldots\ldots\ldots\ldots\ldots\ldots\ldots\ldots\ldots\ldots\ldots\ldots\ldots\ldots\ldots\ldots\ldots \\ H_{mn}(M\,(j\omega_n)^2 + L\,(j\omega_n) + K)H_{mn} = H_{mn} + \Delta_n(M\,(j\omega_n)^2 + L\,(j\omega_n) + K)H_{mn} \end{cases} \tag{35}$$

and to solve the new linear least-squares problem with criterion

$$\tilde{J}(M, L, K) = \sum_{i=1}^{n} Trace(\tilde{\Delta}_i^* \tilde{\Delta}_i) \tag{36}$$

where $\tilde{\Delta}_i = \Delta_i(M\,(j\omega_i)^2 + L\,(j\omega_i) + K)H_{mi}$. If M, L, and K can be found such that $\Delta_1, \ldots, \Delta_n$ are small, then $(M\,(j\omega_i)^2 + L\,(j\omega_i) + K)H_{mi} \sim I$ for $i = 1 : n$, so that the new optimization problem is nearly equivalent to the original one. It is however much easier to solve because it is linear.

The optimization of $\tilde{J}$ gives estimates for the dynamic parameters M, L, and K which can be used to start the optimization of J.

7.1.5 Application: Calculated modal frequency response of ASCIE 4-mode-model between 13 and 18 Hz

The above dynamic estimation procedure was applied to the ASCIE 4-mode-subsystem frequency response between 13 and 18 Hz to determine M, L, and K. The corresponding theoretical frequency response is shown in Figure (13) and the fit error is shown in Figure (14).

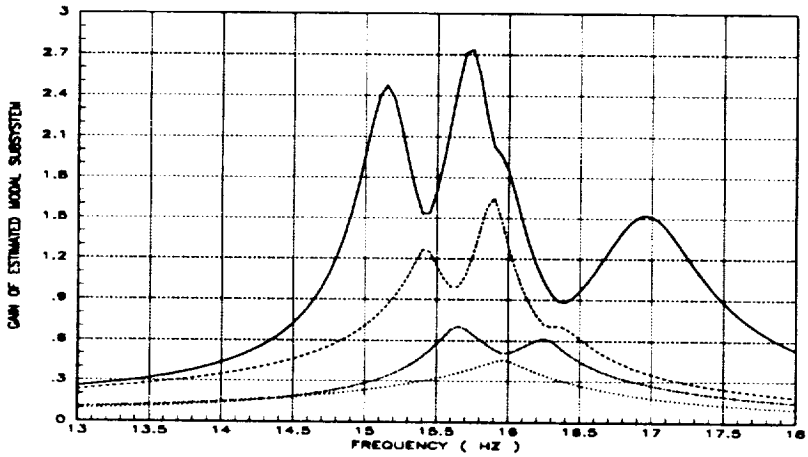

Figure 13: Calculated ASCIE initial 4-mode-model frequency response between 13 and 18 Hz

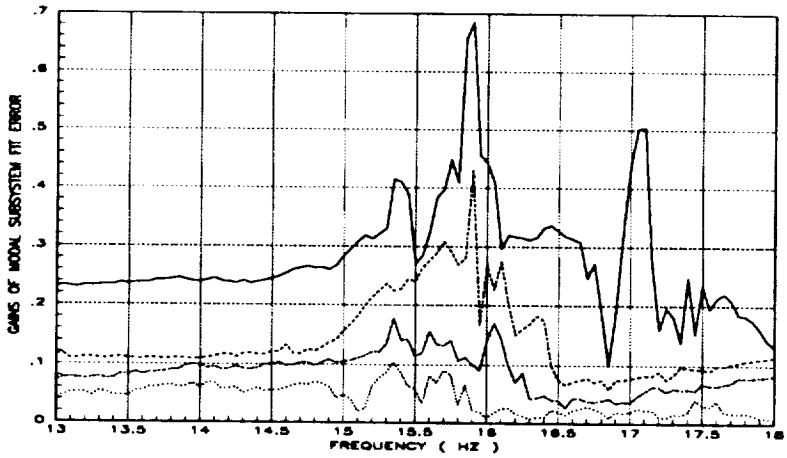

Figure 14: ASCIE initial modal response fit error between 13 and 18 Hz

J was then optimized using an explicit 2nd order Newton-Raphson iterative algorithm and using the above values of M, L, and K as starting parameters. The frequency response of the theoretical modal subsystem and of the corresponding residual subsystem is shown in Figure (15) and Figure (16), respectively.

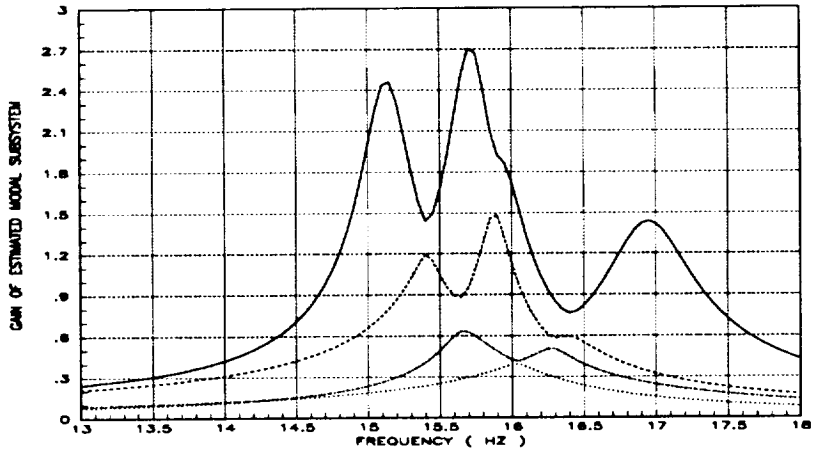

Figure 15: Calculated ASCIE optimal 4-mode-model frequency response between 13 and 18 Hz

7.1.6 Practical comments

This section describes and illustrates the application of new algorithms to extract the modal characteristics of a system from its measured frequency response. In the above example, 4 dominant modes were simultaneously extracted from the colocated frequency response of ASCIE between 13 and 18 Hz. By focusing the analysis on smaller frequency ranges, the same algorithms can be used to extract one mode at a time. At present, the extraction procedure is interactive: the user decides in what frequency range he wants to focus the analysis, and how many modes he wants to extract simultaneously.

We have found it useful to extract a single mode at a time, particularly in high modal density regions. In doing so we gained the assurance that a mode was indeed extracted each time. When to terminate the iterative extraction procedure is a matter of judgement. We always did so when, in any part of the spectrum, the phase of the dominant non parametric modal frequency response varied widely. For instance, Figure (17) shows the residual response of ASCIE between 20 and 29 Hz after 27 modes are extracted. Figure (18) shows the non parametric modal frequency response of the dominant part of the residual frequency response between 25.25 and 25.70 Hz (extracting this non parametric response is always the first step in extracting a mode in our procedure). Although the gain plot seems to indicate the presence of a mode around 25.5 Hz, the phase varies widely. The non parametric frequency response is therefore not the response of a pure mode.

As a last comment, the contribution of the modes already extracted, outside of the frequency range being analyzed, can be removed from the frequency response before starting the analysis. This usually improves the quality of the modal data.

7.2 Modal characterization of ASCIE between 1 and 50 Hz

This section explains how the modal characteristics of the ASCIE segmented optics and support structure between 1 and 50 Hz were obtained from its measured colocated frequency response (Figure (9)).

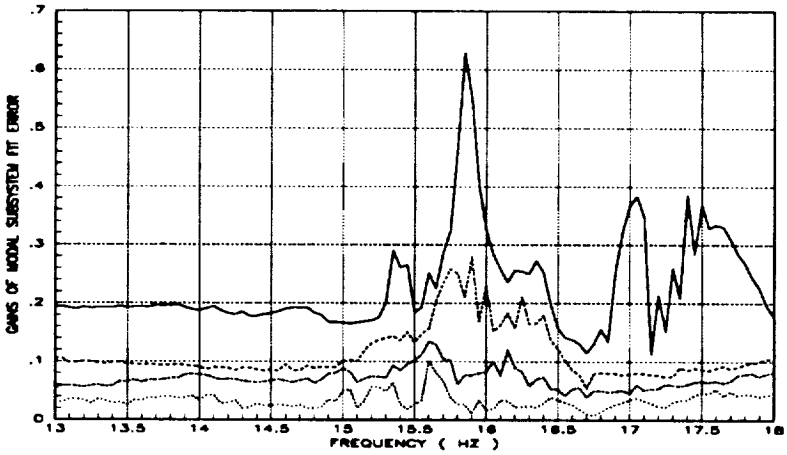

Figure 16: ASCIE optimal modal response fit error between 13 and 18 Hz

The main idea consists in isolating the modes according to their resonant frequencies and according to their mode shapes (spatial separation) to break the global characterization problem into simpler ones. Frequency separation is easy to perform by visual inspection of the system frequency response: the dominant modes with similar frequencies are grouped together. For instance, the ASCIE colocated frequency response was partitioned over 6 frequency ranges: 1 Hz to 13 Hz, 13 Hz to 18 Hz, 20 Hz to 29 Hz, 28 Hz to 33 Hz, 33 Hz to 39 Hz, and 39 Hz to 50 Hz. On each frequency range, when frequency alone failed to isolate modes, spectral and spatial separation was used concurrently: the analytical modal separation algorithms described and illustrated in section 7.1 were used to iteratively extract the modes from the measured frequency response one mode at a time.

8 OFF-LINE DYNAMIC CHARACTERIZATION, ALGORITHMS AND APPLICATION TO ASCIE

In the previous section, simple yet effective algorithms were developed to compute "good" estimates of the modal characteristics of ASCIE from its frequency response. Frequency separation, spatial separation, and modal dominance were used to extract natural modes one at a time. In general, however, it is not possible to exactly differentiate modes. Some of the deficiencies of analytical modal separation are:

- In the process of extracting the natural modes of ASCIE in the high modal density region, we noticed that some modes have close resonant frequencies and similar mode shapes at the actuator or the sensor locations. The algorithms do not guarantee that accurate modal characteristics are determined in this situation.

- If the extraction process of the previous section is iterated too many times in an attempt to extract modes with relatively low modal response, one may end up extracting more modes

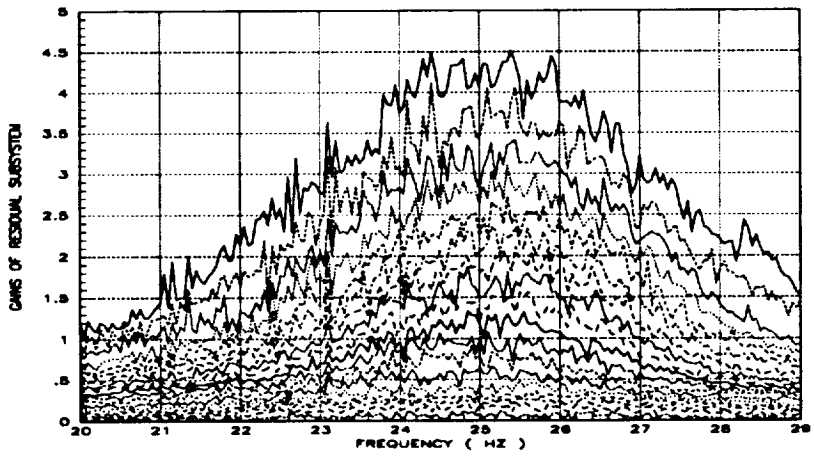

Figure 17: Residual frequency response between 20 and 29 Hz after complete modal extraction

than actually exist in the frequency range being analyzed. For instance, assume that some error is made in calculating the mode shape at the actuator location of a dominant mode whose response is

$$P(s) = g\frac{c\,b}{s^2 + 2\xi\omega s + \omega^2} \tag{37}$$

Let b, $\hat{b}$, and $\Delta b = b - \hat{b}$ be the actual value, the calculated value, and the error associated with the mode shape at the actuator location. Then assuming that all the other modal parameters have been estimated exactly, the residual frequency response once the estimated modal response has been removed will contain a term of the form $\Delta P(s) = g\frac{c\,\Delta b}{s^2+2\xi\omega s+\omega^2}$ which looks like the frequency response of a pure mode with low modal response.

- Analytical modal separation is based on modal dominance, frequency separation, and spatial separation. Consequently, the accuracy of the modal parameters determined applying this method degrades as the contribution of the modes outside of the frequency range being analyzed and of the modes not yet extracted within the frequency range being analyzed, increases.

Because of the above deficiencies, it is possible to improve on the values of the modal parameters of ASCIE determined in the previous section by performing a global analysis of the complete frequency response. In the next sections, we address the problem of extracting the linear dynamics of a system from its measured frequency response by least-squares curve fitting.

8.1 Limitations of current curve fitting techniques

Many algorithms were developed for Single-Input Single-Output (SISO) complex curve fitting problems, and particular attention was paid to eliminating numerical ill-conditioning using various parameterizations [18–20]. Most of them solve the original nonlinear least-squares problem by iteratively solving a frequency reweighted linear least-squares problem. The initialization is similar

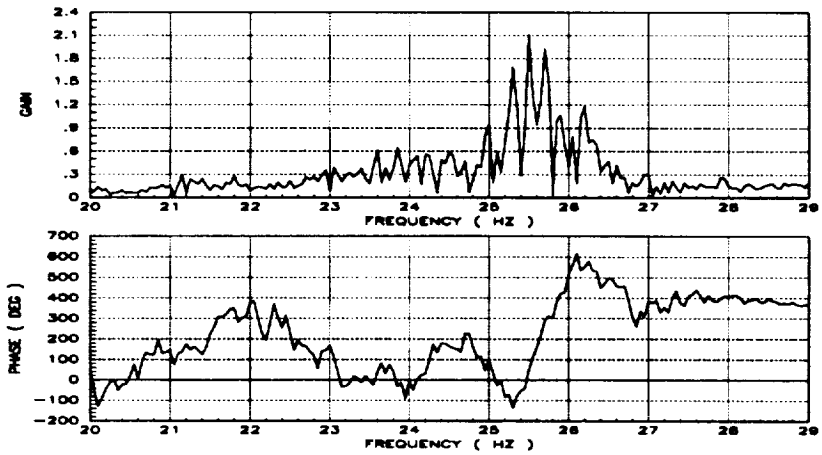

Figure 18: Non parametric frequency response of ASCIE 1-mode-model estimated from the residual frequency response of ASCIE between 25.25 and 25.70 Hz

to the initialization procedure used to estimate the dynamics of a modal system in section 7.1.4. However, because of the particular problem being solved, it was then very easy to restore proper frequency weighting. This is not the case in general SISO problems and this issue may be more important than numerical ill-conditioning. Some of the SISO techniques have been generalized to Single-Input Multiple-Output (SIMO) problems[21], but not to the Multiple-Input Multiple-Output (MIMO) curve fitting problems. At present, MIMO problems are reduced to a series of SIMO problems.

Analytical modal identification techniques and modal test engineers face the same problems. Experimentally, modal testing fails when it becomes impossible to isolate modes on the basis of their frequency separation, spatial separation, and modal dominance. Similarly, the curve fitting problem becomes numerically ill-conditioned under the same conditions. This problem is exacerbated in SISO problems because spatial separation is lost in this case. Although analytical techniques can numerically deal successfully with much more complex systems than the test engineer can experimentally, they cannot deal with the complexity of the ASCIE response in the high modal density regions. To illustrate this point, the frequency response of ASCIE from a single segment alignment actuator to a single edge sensor was plotted in Figure (19). The amplitude response is extremely complex and SISO curve fitting techniques would not be able to differentiate true modes from "noise modes" in this case. The phase plot shows similar complexity. This differentiation problem would still arise, although to a lesser extent, if SIMO responses and SIMO curve fitting techniques were considered.

Even assuming that the 18 SIMO ASCIE identification problems in the high modal density region between 20 and 29 Hz could be solved, one would still be faced with the problem of putting together 18 dynamic models, each of order approximately 40. Eliminating the redundant modes using balanced model order reduction [22] would then require solving Lyapunov equations of order approximately 700 !

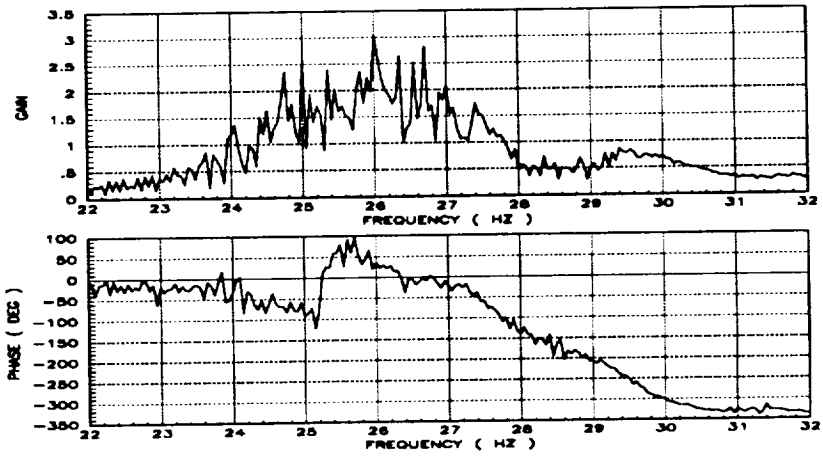

Figure 19: Modal differentiation failure when using classical frequency sweep

8.2 Multiple-Input Multiple-Output curve fitting for ASCIE

In section 7, new algorithms were developed and applied to find what the number of modes and what the modal characteristics of ASCIE are on 6 different frequency ranges. 6 modal subsystems were thus identified. These models can now be used to initialize a global optimization procedure. The objective of this section is to combine these 6 modal subsystems and to correct for the deficiencies of analytical modal separation techniques. This is done in two steps. In the first step, further analysis is performed on each frequency range to reduce the difference between the measured and the theoretical modal responses and if possible reduce the order of the corresponding modal subsystem. In the second step, the various models are combined and a global optimization of the least-squares cost function is attempted. In the following section, we describe the optimization strategy used first to optimize the 6 modal subsystems on their respective frequency range, and next to optimize the combined subsystems.

8.2.1 Subset parameter optimization

Let the theoretical transfer function matrix of a general damped oscillatory system be:

$$H(s) = (C_1 + s\,C_2)\,(s^2 I + 2\xi\Omega s + \Omega^2)^{-1}(s\,B_1 + B_2) + D \tag{38}$$

Let $H_1, \ldots, H_n$ be the measured frequency responses, and let $\Delta_1, \ldots, \Delta_n$ be the differences between the measured and the theoretical responses at the frequencies $j\omega_1, \ldots, j\omega_n$ respectively. The least-squares identification problem is to find the real matrices $C = [C_1, C_2]$, $B = [B_1, B_2]$, D, and the diagonal matrices $\xi > 0$ and $\Omega > 0$ such that:

$$J(C, B, D, \xi, \Omega) = \sum_{i=1}^{n} Trace(\Delta_i^* \Delta_i) \tag{39}$$

is minimized.

The global minimization of J for large systems is impractical. The length of the parameter vector constructed from the coefficients of B, C, D, ξ, and Ω that would have to be optimized to fit a linear model to the frequency response of ASCIE between 20 and 29 Hz would be over 1800. Brute force explicit 2nd order optimization algorithms would therefore take an excessive amount of computer time to run, and would require more work space than is currently available with most computers.

As an alternative, we propose to successively and iteratively optimize C, B, D, and $[\xi\Omega, \Omega^2]$. The same method was proposed in [23] to solve the model reduction problem which is similar to the present least-squares identification. This method, called parameter subset optimization, operates like the QR algorithm when it is used to find the minimum of a positive definite quadratic form (the QR algorithm finds the optimum by solving a finite number of line searches). Although parameter subset optimization does not enjoy the nice properties of the QR algorithm, we have always found it very efficient in practice.

The choice of the parameter subsets C, B, D, and $[\xi\Omega, \Omega^2]$ takes advantage of the structure of the least-squares identification problem. Since the cost function J is quadratic and convex in C, B, and D respectively, the corresponding optimization problems can be solved explicitly. The most difficult part is to optimize J with respect to $[\xi\Omega, \Omega^2]$. Fortunately, this problem involves relatively few parameters so that an explicit 2nd order Newton-Raphson algorithm can be used.

8.2.2 ASCIE modal subsystem optimization

6 ASCIE modal subsystems were extracted from the measured ASCIE frequency response over 6 different frequency ranges using analytical modal separation. As a first step to improve the accuracy of the modal parameters of each modal subsystem, an attempt is made to get values for the modal parameters free from the influence of the modes that do not belong to the subsystem. Thus, for each of the 6 frequency ranges defined above, the measured ASCIE frequency response was corrected by eliminating the estimated contribution of the modes outside of this frequency range, and the corresponding modal subsystem was optimized to match the residual modal frequency response (assume true modal response) thus calculated. Parameter subset optimization was applied to carry out the optimization.

As a second step, each modal subsystem was screened for possible modal redundancy and reoptimized. Balanced model order reduction was used to eliminate the redundant modes. The model order reduction was stopped when the elimination of any mode would have increased the value of the least-squares cost function by at least 1% . The number of modes of the modal subsystem between 20 and 29 Hz was thus reduced from 27 to 21. The number of modes of the modal subsystem between 33 and 39 Hz was reduced from 13 to 11. The orders of the 4 other subsystems were not reduced. With current SIMO least-squares curve fitting techniques, we would have had to reduce the number of modes of the modal subsystem between 20 and 29 Hz from approximately 18x21=378 to 21, and the number of modes of the modal subsystem between 33 and 39 Hz from approximately 18x13=234 to 11. Our method is more effective because it leads to a much lower modal redundancy.

8.2.3 Combining the modal subsystems

The ASCIE modal subsystems were combined and the resulting model was optimized to match the complete measured ASCIE frequency response using parameter subset optimization. This last step yielded less than a 1% decrease in the least-squares cost function. As for ASCIE, this step may well be unnecessary in many applications.

The frequency response of the identified model after optimization is given in Figure (20), and the corresponding residual response in Figure (21). A list of the identified dynamic parameters is given in Table (2). The first three modes are stand modes.

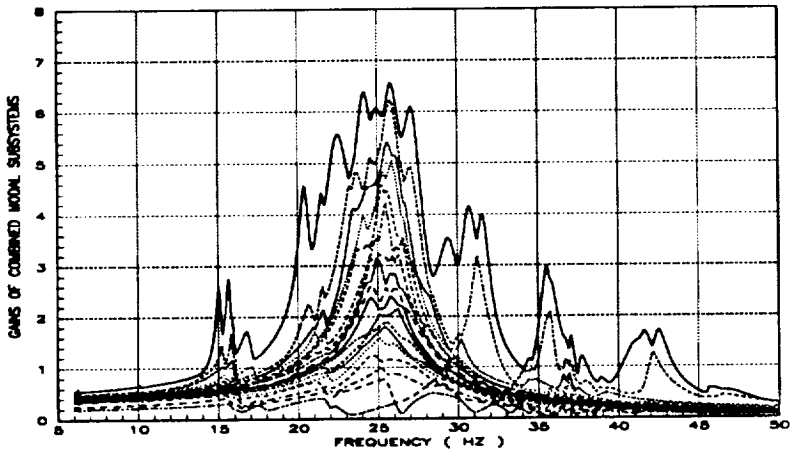

Figure 20: Calculated colocated frequency response of ASCIE

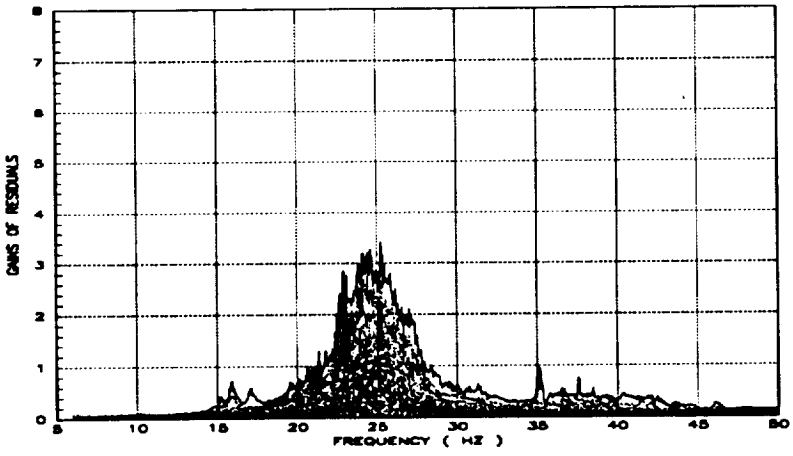

Figure 21: Residual ASCIE colocated frequency response after the optimized modal response is removed

MODE NUMBER	DAMPING %	FREQUENCY (HZ)	MODE NUMBER	DAMPING %	FREQUENCY (HZ)
1	0.90	4.9172	26	2.65	27.0039
2	0.31	6.2855	27	2.30	27.1858
3	0.72	10.1845	28	3.63	27.2201
4	1.28	15.0804	29	2.49	29.5919
5	1.17	15.6929	30	2.03	30.6646
6	1.01	15.9060	31	1.54	31.5755
7	2.30	16.8985	32	0.73	34.5256
8	1.79	20.4568	33	1.20	35.5957
9	1.05	21.5582	34	0.43	35.6220
10	4.21	22.4873	35	1.01	35.7824
11	3.94	23.7036	36	2.07	36.5263
12	4.90	24.0046	37	0.27	36.6676
13	3.31	24.2425	38	0.70	36.7465
14	5.27	24.3552	39	0.48	37.0040
15	2.75	24.3952	40	2.52	37.2631
16	3.80	24.9325	41	0.60	37.5024
17	2.93	24.9918	42	1.06	37.8245
18	7.33	25.2170	43	0.62	38.7592
19	3.18	25.4578	44	2.16	41.1248
20	4.06	25.7026	45	0.83	41.5539
21	2.64	25.8462	46	1.26	42.4540
22	3.42	25.9054	47	0.16	45.6241
23	2.97	25.9286	48	1.13	45.7434
24	3.89	26.1478	49	1.58	46.3683
25	2.78	26.3024	50	2.75	47.6578

Table 2: Modal frequencies and damping ratios of ASCIE 50 mode model

9 CONCLUSION

This paper reports on advances in four areas of system identification of complex flexible structures from frequency responses:

- data acquisition: a method that maintains, to the extent possible, a specified signal to noise ratio is developed to measure frequency responses using sinusoidal test signals.
- on-line modal tuning: an experimental procedure is developed to isolate modes to measure their characteristics on the basis of their spectral separation, spatial separation, and the dominance of their response.
- off-line analytical modal separation: new algorithms are developed to determine the modal characteristics of a system from its measured frequency response on the basis of spectral separation, spatial separation, and modal response dominance.

- curve fitting: a parameter subset optimization method is proposed that takes advantage of the structure of the non linear least-squares identification problem and reduces it to successively and iteratively solving two linear least-squares optimization problems and one non linear least-squares problem of relatively small size. The method can deal with much more complex systems than standard optimization techniques.

The new methods are applied to the modal characterization of the ASCIE segmented optics testbed. They coped successfully with the problem of estimating over 2000 modal parameters, and resolving modal clusters with a modal density of 5 modes/Hz.

The new methods are combined into a constructive system identification procedure that breaks the global modeling problem into smaller ones easier to solve. As a result, they can be used to model systems even more complex than ASCIE which is critical for future applications. They also are suitable for on-orbit modal testing of spacecrafts because they do not require any special purpose instrumentation.

Aknowledgement: The authors would like to thank Ernie Perez, Paul Reshatoff, and Don Zacharie for their outstanding technical support.

A Approximation of a matrix by one of lower rank

Given a matrix H of rank n, the problem is to find a matrix $\hat{H}$ of rank $nr < n$ such that the Euclidian norm of the error $H - \hat{H}$ is minimized. The following theorem holds:

Theorem A.1 *Let $\sum_{i=1}^{n} \sigma_i u_i v_i^T$ be a singular value decomposition of H where $\sigma_1 \geq \sigma_2 \geq \ldots \geq \sigma_n > 0$, then of all the matrices of rank nr, $\hat{H} = \sum_{i=1}^{nr} \sigma_i u_i v_i^T$ is a best approximation of H in the Euclidian norm sense.*

In matrix form, denoting $C = [u_1, \ldots, u_{nr}]$ and $X^T = [\sigma_1 v_1, \ldots, \sigma_{nr} v_{nr}]$, then $\hat{H} = C\ X$ is a best approximation of H of rank nr in the Euclidian norm sense.

B Biased approximation of a matrix by one of lower rank

Given a matrix H of rank n and a full row rank matrix U, the problem is to find a matrix $\hat{H}$ of rank $nr < n$ and a matrix D such that the Euclidian norm of the error $H - (\hat{H} + D\ U)$ is minimized. The following theorem holds:

Theorem B.1 *Let $U^{\perp}$ be an orthogonal complement of U ($U^{\perp} U^{\perp T} = I$ and $U\ U^{\perp T} = 0$). Let $\sum_{i=1}^{n} \sigma_i u_i v_i^T$ be a singular value decomposition of $H\ U^{\perp T}$ where $\sigma_1 \geq \sigma_2 \geq \ldots \geq \sigma_n \geq 0$, then, of all the matrices of rank nr, $\hat{H} = (\sum_{i=1}^{nr} \sigma_i u_i v_i^T) U^{\perp}$ is a best biased approximation of H in the Euclidian norm sense. The bias matrix coefficient D is then $D = H\ U^T (U\ U^T)^{-1}$.*

Proof: Any matrix $\hat{H}$ of rank nr can be written as the product of two full rank matrices C and X of rank nr:

$$\hat{H} = C\ X \tag{40}$$

The problem is to find C, X, and D to minimize:

$$J = Trace\left[(H - (C\,X + D\,U))^T(H - (C\,X + D\,U))\right] \tag{41}$$

The optimization problem is convex in C, X, and D respectively, but not with respect to C and X simultaneously.

Since

$$\begin{aligned} X &= X\,(I - U^T(U\,U^T)^{-1}U) + X\,U^T(U\,U^T)^{-1}U \\ &= X\,U^{\perp T}U^{\perp} + X\,U^T(U\,U^T)^{-1}U \end{aligned}$$

we have:

$$C\,X + D\,U = C\,X\,U^{\perp T}U^{\perp} + (D + X\,U^T(U\,U^T)^{-1})\,U \tag{42}$$

We can therefore assume without loss of generality that $X\,U^T = 0 \quad \Leftrightarrow \quad X = X_1 U^{\perp}$ for some X_1. The first order condition of optimality with respect to D then gives:

$$D = H\,U^T(U\,U^T)^{-1} \tag{43}$$

which is independent of both C and X !

The cost function J then becomes:

$$J = Trace\left[(H\,U^{\perp T} - C\,X_1)^T(H\,U^{\perp T} - C\,X_1)\right] \tag{44}$$

The problem is now to approximate $H\,U^{\perp T}$ by a matrix of rank nr. Its solution is a simple application of the theorem of Appendix A.

□

Remark B.1 *It can be shown that, generically, C is unique up to an invertible right transformation.*

C Relationship between the modal and the physical dynamic equations of an oscillatory system

In this section, we show that the dynamic equations of a system with nonproportional damping, force commands, and position measurements can indeed equivalently be rewritten in the modal form postulated in section 5.2.

Rewrite the dynamic equations of the system (2) in first order form:

$$\begin{bmatrix} \dot{z} \\ \ddot{z} \end{bmatrix} = \begin{bmatrix} 0 & I \\ -M^{-1}K & -M^{-1}L \end{bmatrix} \begin{bmatrix} z \\ \dot{z} \end{bmatrix} + \begin{bmatrix} 0 \\ M^{-1}E \end{bmatrix} u + \begin{bmatrix} 0 \\ M^{-1} \end{bmatrix} d \tag{45}$$

and define the state space transformation $V = \begin{bmatrix} V_1 & V_{12} \\ V_{21} & V_2 \end{bmatrix}$:

$$\begin{bmatrix} z \\ \dot{z} \end{bmatrix} = \begin{bmatrix} V_1 & V_{12} \\ V_{21} & V_2 \end{bmatrix} \begin{bmatrix} x_1 \\ x_2 \end{bmatrix} \tag{46}$$

such that:

$$\begin{bmatrix} 0 & I \\ -M^{-1}K & -M^{-1}L \end{bmatrix} \begin{bmatrix} V_1 & V_{12} \\ V_{21} & V_2 \end{bmatrix} = \begin{bmatrix} V_1 & V_{12} \\ V_{21} & V_2 \end{bmatrix} \begin{bmatrix} 0 & I \\ -\Omega^2 & -2\,\xi\,\Omega \end{bmatrix} \tag{47}$$

The dynamic equations of the system can then equivalently be rewritten:

$$\begin{cases} \begin{bmatrix} \dot{x_1} \\ \dot{x_2} \end{bmatrix} = \begin{bmatrix} 0 & I \\ -\Omega^2 & -2\,\xi\,\Omega \end{bmatrix} \begin{bmatrix} x_1 \\ x_2 \end{bmatrix} + \begin{bmatrix} \bar{B}_1 \\ \bar{B}_2 \end{bmatrix} u + \begin{bmatrix} \bar{B}_{d1} \\ \bar{B}_{d2} \end{bmatrix} d \\ y = \begin{bmatrix} \bar{C}_1 & \bar{C}_2 \end{bmatrix} \begin{bmatrix} x_1 \\ x_2 \end{bmatrix} + e \end{cases} \tag{48}$$

where we have defined:

$$\begin{cases} \left[\begin{array}{c|c} \bar{B}_1 & \bar{B}_{d1} \\ \bar{B}_2 & \bar{B}_{d2} \end{array}\right] = \begin{bmatrix} V_1 & V_{12} \\ V_{21} & V_2 \end{bmatrix}^{-1} \left[\begin{array}{c|c} 0 & 0 \\ -M^{-1}E & -M^{-1} \end{array}\right] \\ \begin{bmatrix} \bar{C}_1 & \bar{C}_2 \end{bmatrix} = \begin{bmatrix} S & 0 \end{bmatrix} \begin{bmatrix} V_1 & V_{12} \\ V_{21} & V_2 \end{bmatrix} \end{cases} \tag{49}$$

From the last set of differential equations, we find:

$$\begin{cases} \ddot{x}_1 + 2\,\xi\,\Omega\,\dot{x}_1 + \Omega^2 x_1 = \bar{B}_1\dot{u} + (\bar{B}_2 + 2\,\xi\Omega\bar{B}_1)u + \bar{B}_{d1}\dot{d} + (\bar{B}_{d2} + 2\,\xi\Omega\bar{B}_{d1})d \\ y = \bar{C}_1 x_1 + \bar{C}_2\dot{x}_1 - \bar{C}_2\bar{B}_1 u - \bar{C}_2\bar{B}_{d1}d + e \end{cases} \tag{50}$$

That is a set of equations identical to the postulated modal equations (11) if we define:

$$\begin{cases} q = x_1 \\ \left[\begin{array}{c|c} B_1 & B_{d1} \\ B_2 & B_{d2} \end{array}\right] = \left[\begin{array}{c|c} \bar{B}_1 & \bar{B}_{d1} \\ \bar{B}_2 + 2\,\xi\Omega\bar{B}_1 & \bar{B}_{d2} + 2\,\xi\Omega\bar{B}_{d1} \end{array}\right] \\ \begin{bmatrix} C_1 & C_2 & D & D_d \end{bmatrix} = \begin{bmatrix} \bar{C}_1 & \bar{C}_2 & -\bar{C}_2\bar{B}_1 & -\bar{C}_2\bar{B}_{d1} \end{bmatrix} \end{cases} \tag{51}$$

Furthermore these equations yield the constraints (12) as follows:

$$\begin{cases} D = -C_2 B_1 \\ D_d = -C_2 B_{d1} \\ C_1 B_1 + C_2(B_2 - 2\xi\Omega B_1) = \bar{C}_1\bar{B}_1 + \bar{C}_2\bar{B}_2 = \begin{bmatrix} S & 0 \end{bmatrix} V\,V^{-1} \begin{bmatrix} 0 \\ M^{-1}E \end{bmatrix} = 0 \\ C_1 B_{d1} + C_2(B_{d2} - 2\xi\Omega B_{d1}) = \bar{C}_1\bar{B}_{d1} + \bar{C}_2\bar{B}_{d2} = \begin{bmatrix} S & 0 \end{bmatrix} V\,V^{-1} \begin{bmatrix} 0 \\ M^{-1} \end{bmatrix} = 0 \end{cases} \tag{52}$$

Unicity The dynamic of a system with non proportional damping can equivalently be described by many different sets of modal equations. One convenient way to parameterize all the possible sets of modal equations that describe a given system is to introduce three complex matrices

$$\begin{cases} B = B_r + j\,B_i \\ B_d = B_{dr} + j\,B_{di} \\ C = C_r + j\,C_i \end{cases} \tag{53}$$

and to rewrite the modal equations as follows:

$$\begin{cases} \ddot{q} + 2\,\xi\,\Omega\,\dot{q} + \Omega^2 q = B_i\dot{u} + (\xi\Omega B_i + \sqrt{I-\xi^2}\Omega B_r)u + B_{di}\dot{d} + (\xi\Omega B_{di} + \sqrt{I-\xi^2}\Omega B_{dr})d \\ y = (C_r\sqrt{I-\xi^2}\Omega + C_i\xi\Omega)q + C_i\dot{q} - C_iB_iu - C_iB_{di}d + e \end{cases} \tag{54}$$

For a system with force commands and position measurements the constraints then become:

$$\begin{cases} C_rB_i + C_iB_r = 0 \\ C_rB_{di} + C_iB_{dr} = 0 \end{cases} \tag{55}$$

The rows of B are then the complex mode shapes at the actuator locations, the rows of B_d the complex mode shapes at the node locations, and the columns of C the complex mode shapes at the sensor locations.

It can be shown that any two sets of modal equations with complex mode shapes (B, B_d, C), and ($\bar{B}$, $\bar{B}_d$, $\bar{C}$) respectively describe the same physical system if and only if there exists a complex diagonal and non singular matrix α such that:

$$\begin{cases} B = \alpha\,\bar{B} \\ B_d = \alpha\,\bar{B}_d \\ C = \bar{C}\,\alpha^{-1} \end{cases} \tag{56}$$

Complex mode shapes are thus defined up to a complex scalar multiplication. This limits significantly their usefulness in practice.

References

[1] Lorell K., Aubrun J-N., Zacharie D., Perez E., 'Development of a Precision, Wide-Dynamic-Range Actuator For Use In Active Optical Systems', Proc. 23rd Aerospace Mechanisms Symposium, pp. 139–156, 1989.

[2] Stroud R., Bonner C., Chambers G., 'Modal Testing Options for Spacecraft Developments', Society of Automotive Engineers Transactions, 1978.

[3] Moonen M., VanDerValle J., 'QSVD Approach to On and Off-Line State Space Identification', International Journal of Control, Vol. 51, no. 5, 1990.

[4] Juang J., Pappa R., 'An Eigenvalue Realization Algorithm for Modal Parameter Identification and Model Reduction', Journal of Guidance, Control and Dynamics, Vol. 8, pp. 620–627, Sept.-Oct. 1985.

[5] Allemang R., Shelley S., Brown D., Zhang Q., 'Practical Experience with Identification of Large Flexible Structures', Proceedings of the American Control Conference, 1991.

[6] Bayard D., Hadaegh F., Yan Y., Scheid R., Mettler E., Milman M., 'Frequency Domain Identification Experiment on a Large Flexible Structure', Proceedings of the American Control Conference, 1990.

[7] Stroud R., Smith S., Hamma G., 'MODALAB - A New System of Structure Dynamic Testing', The Shock and Vibration Bulletin, No. 46, pp. 153–175, August 1976.

[8] Asher G., 'A Method of Normal Mode Excitation Utilizing Admittance Measurements', Proceedings of the National Specialists' Meeting on Dynamics and Aeroelasticity, pp. 69–76, Forth Worth, Texas, November 1958.

[9] Smith S., Woods A., 'A Multiple Driver Admittance Technique for Vibration Testing of Complex Structures', The Shock and Vibration Bulletin, No. 42, Part 3, January 1972.

[10] Balas G., Doyle J., 'Identification for Robust Control of Flexible Structures', Proceedings of the American Control Conference, 1990.

[11] Anderson B.D.O., Antoulas A., 'Rational Interpolation and State-Space Realizations', Proceedings of the 29th Conference on Decision and Control, Hawaii, December 1990.

[12] Gu G., Khargonekar P., 'Linear and Nonlinear Algorithms for Identification in H_∞ with Error Bounds', Proceedings of the American Conference, June 1991.

[13] Gu G., Misra P., 'Identification of Linear Time-Invariant Systems', Proceedings of the American Control Conference, June 1991.

[14] Lewis R., Wrisley D., 'A system for excitation of pure natural modes of complex structures', Journal of Aerospace Sciences, Vol. 17, No. 11, pp. 705–722, November 1950.

[15] Ibanez P., 'Force Appropriation by Extended Asher's Method', presented at the SAE Aerospace Engineering and Manufacturing Meeting, San Diego, CA, December 1976.

[16] Ryan R. et al., 'Dynamic Testing for Large Systems', NASA TM-78307, Sept. 1980.

[17] Golub G., Van Loan C., *Matrix computations*, 1983, Hopkins.

[18] Levy E., 'Complex Curve Fitting', IRE Transactions on Automatic Control, Vol. AC-4, May 1959, pp. 37–44.

[19] Spanos J., Mingori D., 'A Newton Algorithm for Complex Curve Fitting', Proceedings of the American Control Conference, Boston, MA, June 1991.

[20] Adcock J., 'Curve fitter for pole-zero analysis', Hewlett-Packard Journal, January 1987.

[21] Dailey R., Lukich M., 'MIMO transfer function curve fitting using Chebyschev polynomials', SIAM 35th Anniversary Meeting, Denver, Colorado, 1987.

[22] Moore B., 'Principal Component Analysis in Linear Systems: Controllability, Observability, and Model Reduction', IEEE Transactions on Automatic Control, AC 26, No. 1, Feb. 1981.

[23] Carrier A., 'Modeling and Shape Control of a Segmented-Mirror-Telescope', Stanford University PhD Thesis, Department of Aeronautics and Astronautics, March 1990.